

Be More Diverse than the Most Diverse: Online Selection of Diverse Mixtures of Generative Models

Parham Rezaei*, Farzan Farnia[†], Cheuk Ting Li[‡]

The availability of multiple training algorithms and architectures for generative models requires a selection mechanism to form a single model over a group of well-trained generation models. The selection task is commonly addressed by identifying the model that maximizes an evaluation score based on the diversity and quality of the generated data. However, such a best-model identification approach overlooks the possibility that a mixture of available models can outperform each individual model. In this work, we explore the selection of a mixture of multiple generative models and formulate a quadratic optimization problem to find an optimal mixture model achieving the maximum of kernel-based evaluation scores including kernel inception distance (KID) and Rényi kernel entropy (RKE). To identify the optimal mixture of the models using the fewest possible sample queries, we propose an online learning approach called *Mixture Upper Confidence Bound (Mixture-UCB)*. Specifically, our proposed online learning method can be extended to every convex quadratic function of the mixture weights, for which we prove a concentration bound to enable the application of the UCB approach. We prove a regret bound for the proposed Mixture-UCB algorithm and perform several numerical experiments to show the success of the proposed Mixture-UCB method in finding the optimal mixture of text-based and image-based generative models. The codebase is available at <https://github.com/rezaei-parham/mixture-ucb>.

1 Introduction

The rapid advancements in generative modeling have created a need for mechanisms to combine multiple well-trained generative models, each developed using different algorithms and architectures, into a single unified model. A common approach for creating such a unified model is to evaluate assessment scores that quantify the diversity and quality of the generated data and then select the model with the highest score. This best-model identification strategy has been widely adopted for the selection of generative models across various domains, including image, text, audio, and video generation.

Existing model selection frameworks typically perform an offline selection, where they have access to a sufficiently large number of samples from each generative model and estimate the evaluation score based on these samples. However, in many practical scenarios, generating a large sample set from sub-optimal models can be computationally costly, especially if the evaluator can identify their lack of optimality using fewer samples. In such cases, the evaluator can adopt an online learning approach and frame the problem as a multi-armed bandit (MAB) task. An existing approach is *successive halving* [1, 2, 3],¹ where the models are evaluated using a fixed budget, the worst half of the models are removed, and we repeat the process until one model is left. Also, the recent work by Hu et al. [5] attempts to solve the online model selection problem using an upper confidence bound (UCB) method to identify the generative model with the highest evaluation score. The numerical results in this work indicate the effectiveness of MAB algorithms in reducing sample generation costs from sub-optimal models.

*Department of Computer Engineering, Sharif University of Technology, parham.rezaei@sharif.edu

[†]Department of Computer Science and Engineering, The Chinese University of Hong Kong, farnia@cse.cuhk.edu.hk

[‡]Department of Information Engineering, The Chinese University of Hong Kong, ctli@ie.cuhk.edu.hk

¹[2] focused on applying successive halving on hyperparameter optimization for supervised learning, whereas [3] focused on generative models using maximum mean discrepancy [4] as the score.

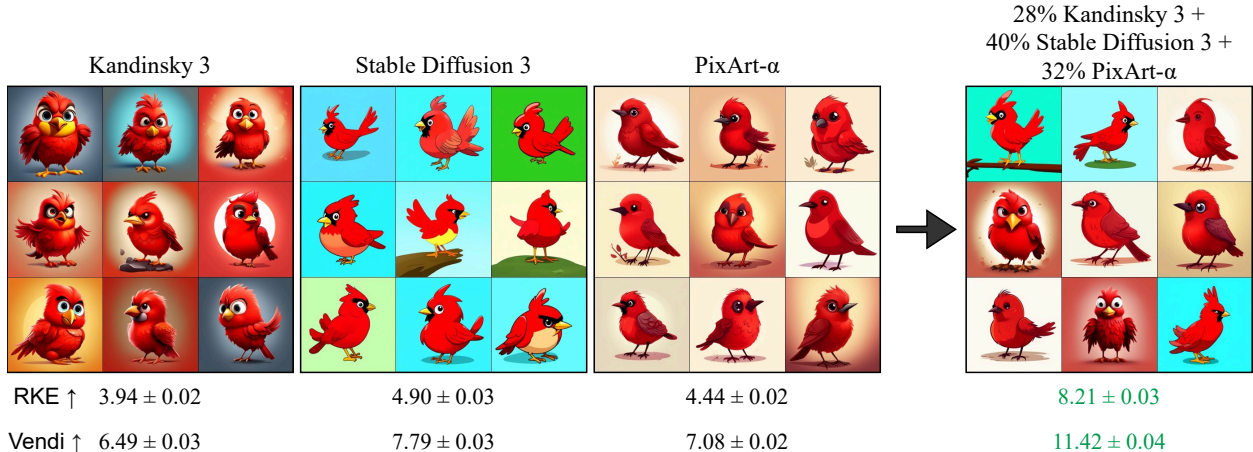


Figure 1: Visual comparison of the diversity across individual arms and the optimal mixture for images generated using models Kandinsky 3, Stable Diffusion 3-medium, and PixArt- α with the prompt "Red bird, cartoon style"

On the other hand, when the model selection task is handled by an online learning algorithm, the algorithm may choose different models at different iterations, resulting in generated data that follow a mixture of the distributions of these generative models. Note that in a standard MAB algorithm, the goal is to eventually converge to a single arm. Successive halving [1, 2, 3] and the standard UCB algorithm adopted by [5] will ultimately select only one generative model after a sufficient number of iterations. However, the diversity scores of the generated data could be higher when the sample generation follows a mixture of models rather than a single model. This observation leads to the following question: could the diversity of generated data be improved by applying MAB algorithms to multiple generative models, if the algorithm aims to find the best mixture of the models?

In this work, we aim to address the above question by finding the optimal mixture $\sum_{i=1}^m \alpha_i P_i$ of m generative models with distributions P_1, \dots, P_m , which would produce a higher evaluation score compared to each individual model. Specifically, we focus on addressing this task in an online learning setting, where we pick a model to generate a sample at each round. To address this problem and develop an MAB algorithm to find the best mixture model, we concentrate on evaluation scores that are quadratic functions of the generated data. As we show in this work, formulating the optimization problem for a quadratic score function results in a quadratic online convex optimization problem that can be efficiently solved using the online gradient descent algorithm. More importantly, we establish a concentration bound for the quadratic function of the mixture weights, which enables us to extend the UCB algorithm for the online selection of the mixture weights.

Specifically, we focus on evaluation scores that reduce to a quadratic function of the generative model's distribution, including the kernel-based Maximum Mean Discrepancy (MMD) [4], Kernel Inception Distance (KID) [6] and Rényi Kernel Entropy (RKE) [7] scores, as well as the quality-measuring Precision [8, 9] and Density [10] scores, which are linear functions of the generative distribution. Among these scores, RKE provides a reference-free entropy function for assessing the diversity of generated data, making it suitable for quantifying the variety of generated samples. Our mixture-based online learning framework can therefore be applied to find the mixture model with the maximum RKE-based diversity score. Additionally, we can consider a linear combination of RKE with the Precision, Density, or KID quality scores to identify a mixture of models that offers the best trade-off between quality and diversity.

We perform several numerical experiments to test the application of our proposed Mixture-UCB approach in comparison to the Vanilla-UCB and One-Arm Oracle approaches that tend to generate samples from only one of the available generative models. Our numerical results indicate that the Mixture-UCB algorithms can generate samples with higher RKE diversity scores, and tends to generate samples from a mixture of

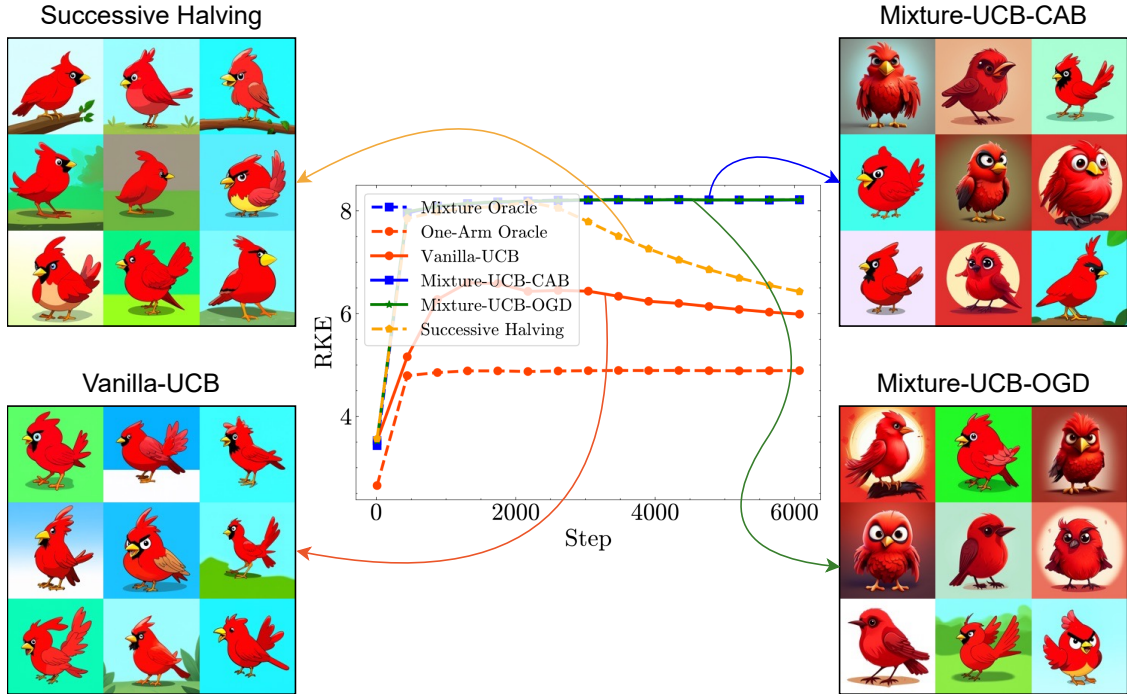


Figure 2: Comparison of our proposed algorithms Mixture-UCB-CAB and Mixture-UCB-OGD with the baseline one arm online algorithms. We plot the diversity-measuring RKE score of the generated data and display 9 (randomly-selected) samples produced in the process of each algorithm.

several generative models when applied to image-based generative models. Also, we test the performance of Mixture-UCB on the KID, Precision, and Density scores, which similarly result in a higher score value for the mixture model found by the Mixture-UCB algorithm. We implement the Mixture-UCB by solving the convex optimization sub-problem at every iteration and also by applying the online gradient descent algorithm at every iteration. In our experiments, both implementations result in satisfactory results and can improve upon learning strategies tending to select only one generative model. The following is a summary of the contributions in this work:

- Studying the selection task for mixtures of multiple generative models to improve the diversity of generated samples.
- Proposing an online learning framework to address the mixture selection task for quadratic score functions.
- Developing the Mixture-UCB-CAB and Mixture-UCB-OGD algorithms to solve the formulated online learning problem.
- Proving a finite horizon regret bound for Mixture-UCB-CAB which shows the convergence of Mixture-UCB-CAB to the optimal mixture.
- Designing the Sparse-Mixture-UCB-CAB algorithm for the situation where we want to eventually select a small subset of the models. This is deferred to Appendix B.
- Presenting numerical results on the improvements in the diversity of generated data by the online selection of a mixture of the generation models.

2 Related Work

Assessment of Generative Models. The evaluation of generative models has been extensively studied, with a focus on both diversity and quality of generated images. Reference-free metrics such as Rényi Kernel Entropy (RKE) [7], VENDI [11], and the FKEA-VENDI [12] measure diversity without relying on ground-truth, while reference-based metrics such as Recall [9] and Coverage [10] assess diversity relative to real data. For image quality evaluation, Density and Precision metrics [9, 10] provide measures based on alignment with a reference distribution. The Wasserstein distance [13] and Fréchet Inception Distance (FID) [14] approximate the distance between real and generated datasets, while Kernel Inception Distance (KID) [6] uses squared maximum mean discrepancy for a kernel-based comparison of distributions. Also, the kernel-based KEN score [15] measures the novelty of generated samples produced by a generative model based on the entropy of their generated sample after canceling the mode-based diversity of a reference distribution.

Multi-Armed Bandit Algorithms. The Multi-Armed Bandit (MAB) problem is a foundational topic in reinforcement learning, where an agent aims to maximize rewards from multiple options (arms) with initially unknown reward distributions [16, 17]. The Upper Confidence Bound (UCB) algorithm [18, 19, 20] is a widely adopted method for addressing the MAB problem, where uncertainty about an arm’s reward is replaced by an optimistic estimate. In generative models, optimism-based bandits have been applied to efficiently identify models with optimal Fréchet Inception Distance (FID) or Inception Score while minimizing data queries [5]. A special case of MAB, the continuum-armed bandit (CAB) problem [21], optimizes a function over continuous inputs, and has been applied to machine learning tasks such as hyperparameter optimization [22, 23]. Recent research explores CABs under more general smoothness conditions like Besov spaces [24], while other works have focused on regret bounds and Lipschitz conditions [25, 26, 27].

Another related reference is informational multi-armed bandits [28], which extends UCB to maximizing the Shannon entropy of a discrete distribution, which is also a metric of diversity. In comparison, the algorithms in this paper can minimize the expectation of any quadratic positive semidefinite function, which not only covers the order-2 Rényi entropy for discrete distributions, but also includes the Rényi Kernel Entropy applicable to continuous data. Since the outputs of generative models are generally continuous, [28] is not applicable here. We also note that the recent paper [29] designs a contextual bandit algorithm for the online prompt-based selection of text-guided generative models, where the online learning algorithm adapts the selection of text-based generative models based on their UCB-estimated relevance CLIPScore in response to the current prompt. We note that our work studies a different online learning setting where the goal is to maximize the score of the mixture of unconditional generative models without any input text prompt.

3 Preliminaries

We review several kernel-based performance metrics of generative models.

3.1 Rényi Kernel Entropy

The *Rényi Kernel Entropy* [7] of the distribution P , which measures the diversity of the modes in P , is given by $\log(1/\mathbb{E}_{X, X' \stackrel{\text{iid}}{\sim} P}[k^2(X, X')])$, where k is a positive definite kernel.² Taking the exponential of the Rényi Kernel Entropy, we have the *RKE mode count* $1/\mathbb{E}[k^2(X, X')]$ [7], which is an estimate of the number of modes. Maximizing the RKE mode count is equivalent to minimizing the following loss

$$\mathbb{E}_{X, X' \stackrel{\text{iid}}{\sim} P}[k^2(X, X')]. \tag{1}$$

²The order-2 Rényi entropy for discrete distributions is a special case by taking $k(x, x') = \mathbf{1}_{x=x'}$.

3.2 Maximum Mean Discrepancy and Kernel Inception Distance

The (squared) *maximum mean discrepancy* (MMD) [4] between distributions P, Q , which measures the distance between P and Q , can be written as

$$\mathbb{E}[k(X, X')] + \mathbb{E}[k(Y, Y')] - 2\mathbb{E}[k(X, Y)], \quad (2)$$

where $X, X' \stackrel{\text{iid}}{\sim} P$ and $Y, Y' \stackrel{\text{iid}}{\sim} Q$, and k is a positive definite kernel. Suppose P is the distribution of samples from a generative model, and Q is a reference distribution. Minimizing the MMD can ensure that P is close to Q . The *Kernel Inception Distance* (KID) [6], a popular quality metric for image generative models, is obtained by first passing P and Q through the Inception network [30], and then computing their MMD, i.e., we have

$$\mathbb{E}[k(\psi(X), \psi(X'))] + \mathbb{E}[k(\psi(Y), \psi(Y'))] - 2\mathbb{E}[k(\psi(X), \psi(Y))], \quad (3)$$

where ψ is the mapping from x to its Inception representation.

4 Optimal Mixtures of Generative Models

RKE (1), MMD (2) and KID (3) can all be written as a loss function in the following form

$$L(P) := \mathbb{E}_{X, X' \stackrel{\text{iid}}{\sim} P}[\kappa(X, X')] + \mathbb{E}_{X \sim P}[f(X)], \quad (4)$$

where $\kappa : \mathcal{X}^2 \rightarrow \mathbb{R}$ is a positive semidefinite kernel, and $f : \mathcal{X} \rightarrow \mathbb{R}$ is a function. For (1), we take $\kappa(x, x') = k^2(x, x')$ (the square of a kernel is still a kernel) and $f(x) = 0$. For (2), we take $\kappa(x, x') = k(x, x')$ and $f(x) = -2\mathbb{E}_{Y \sim Q}[k(x, Y)]$ (the constant term $\mathbb{E}[k(Y, Y')]$ does not matter). For KID (3), we take $\kappa(x, x') = k(\psi(x), \psi(x'))$ and $f(x) = -2\mathbb{E}_{Y \sim Q}[k(\psi(x), \psi(Y))]$. Note that any convex combinations of (1), (2) and (3) is still in the form (4).

Suppose we are given m generative models, where model i generates samples from the distribution P_i . If our goal is merely to find the model that minimize the loss (4), we should select $\text{argmin}_i L(P_i)$. Nevertheless, for diversity metrics such as RKE, it is possible that a mixture of the models will give a better diversity. Assume that the mixture weight of model i is $\alpha_i \in [0, 1]$, where $\boldsymbol{\alpha} = (\alpha_1, \dots, \alpha_m)$ is a probability vector. The loss of the mixture distribution $\sum_{i=1}^m \alpha_i P_i$ can then be expressed as

$$L(\boldsymbol{\alpha}) := L\left(\sum_{i=1}^m \alpha_i P_i\right) = \boldsymbol{\alpha}^\top \mathbf{K} \boldsymbol{\alpha} + \mathbf{f}^\top \boldsymbol{\alpha},$$

$$\mathbf{K} := (\mathbb{E}_{X \sim P_i, X' \sim P_j}[\kappa(X, X')])_{i, j \in [m]} \in \mathbb{R}^{m \times m}, \quad \mathbf{f} := (\mathbb{E}_{X \sim P_i}[f(X)])_{i=1}^m \in \mathbb{R}^m.$$

Given \mathbf{K}, \mathbf{f} , the probability vector $\boldsymbol{\alpha}$ minimizing $L(\boldsymbol{\alpha})$ can be found via a convex quadratic program.

In practice, we do not know the precise \mathbf{K}, \mathbf{f} , and have to estimate them using samples. Suppose we have the samples $x_{i,1}, \dots, x_{i,n_i}$ from the distribution P_i for $i = 1, \dots, m$, where n_i is the number of observed samples from model i . Write $\mathbf{x} := (x_{i,a})_{i \in [m], a \in [n_i]}$. We approximate the true mixture distribution $\sum_{i=1}^m \alpha_i P_i$ by the empirical mixture distribution $\sum_{i=1}^m \frac{\alpha_i}{n_i} \sum_{a=1}^{n_i} \delta_{x_{i,a}}$, where we assign a weight α_i/n_i to samples $x_{i,a}$ from model i , and $\delta_{x_{i,a}}$ denotes the degenerate distribution at $x_{i,a}$. We then approximate $L(\boldsymbol{\alpha})$ by the sample loss

$$\hat{L}(\boldsymbol{\alpha}; \mathbf{x}) := L\left(\sum_{i=1}^m \frac{\alpha_i}{n_i} \sum_{a=1}^{n_i} \delta_{x_{i,a}}\right) = \boldsymbol{\alpha}^\top \hat{\mathbf{K}}(\mathbf{x}) \boldsymbol{\alpha} + \hat{\mathbf{f}}(\mathbf{x})^\top \boldsymbol{\alpha}, \quad (5)$$

$$\hat{\mathbf{K}}(\mathbf{x}) := \left(\frac{1}{n_i n_j} \sum_{a=1}^{n_i} \sum_{b=1}^{n_j} \kappa(x_{i,a}, x_{j,b})\right)_{i, j} \in \mathbb{R}^{m \times m}, \quad \hat{\mathbf{f}}(\mathbf{x}) := \left(\frac{1}{n_i} \sum_{a=1}^{n_i} f(x_{i,a})\right)_{i=1}^m \in \mathbb{R}^m.$$

The minimization of $\hat{L}(\boldsymbol{\alpha}; \mathbf{x})$ over probability vectors $\boldsymbol{\alpha}$ is still a convex quadratic program.

5 Online Selection of Optimal Mixtures – Mixture Multi-Armed Bandit

Suppose we are given m generative models, but we do not have any prior information about them. Our goal is to use these models to generate a collection of samples $(x^{(t)})_{i \in [T]}$ in T rounds that minimizes the loss (4) $L(\hat{P}^{(T)})$ at the empirical distribution $\hat{P}^{(T)} = T^{-1} \sum_{t=1}^T \delta_{x^{(t)}}$. We have

$$L(\hat{P}^{(T)}) = \frac{1}{T^2} \sum_{s,t \in [T]} \kappa(x^{(s)}, x^{(t)}) + \frac{1}{T} \sum_{t=1}^T f(x^{(t)}).$$

If we are told by an oracle the optimal mixture α^* that minimizes the loss $L(\alpha)$, then we should generate samples according to this mixture distribution, giving $\approx \alpha_i^* T$ samples from model i . We call this the *mixture oracle* scenario. Nevertheless, in reality, we do not know \mathbf{K}, \mathbf{f} , and cannot compute α^* exactly. Instead, we have to approximate α^* by minimizing the sample loss $\hat{L}(\alpha; \mathbf{x})$ (5). However, we do not have the samples \mathbf{x} at the beginning in order to compute $\hat{L}(\alpha; \mathbf{x})$, so we have to generate some samples first. Yet, to generate these initial samples, we need an estimate of α^* , or else those samples may have a suboptimal empirical distribution and affect our final loss $L(\hat{P}^{(T)})$, or we will have to discard those initial samples which results in wastage.

This “chicken and egg” problem is naturally solved by an online learning approach via multi-armed bandit. At time $t = 1, \dots, T$, we choose and pull an arm $b^{(t)} \in [m]$ (i.e., generate a sample from model $b^{(t)}$), and obtain a sample $x^{(t)}$ from the distribution $P_{b^{(t)}}$. The choice $b^{(t)}$ can depend on all previous samples $x^{(1)}, \dots, x^{(t-1)}$. Unlike conventional multi-armed bandit where the goal is to maximize the total reward over T rounds, here we minimize the loss $L(\hat{P}^{(T)})$ which involve cross terms $\kappa(x^{(s)}, x^{(t)})$ between samples at different rounds. Note that if $\kappa(x, x') = 0$, then this reduces to the conventional multi-armed bandit setting by taking $f(x)$ to be the negative reward of the sample x . In the following subsections, we will propose two new algorithms that are generalizations of the upper confidence bound (UCB) algorithm for multi-armed bandit [18, 19].

5.1 Mixture Upper Confidence Bound – Continuum-Armed Bandit

Let $n_i^{(t)}$ be the number of times arm i has been pulled up to time t . Let $\mathbf{x}^{(t)} := (x_{i,a})_{i \in [m], a \in [n_i^{(t)}]}$ be the observed samples up to time t . We focus on bounded loss functions, and assume that $\kappa : \mathcal{X}^2 \rightarrow [\kappa_0, \kappa_1]$ and $f : \mathcal{X} \rightarrow [f_0, f_1]$ are bounded. Let $\Delta_\kappa := \kappa_1 - \kappa_0$, $\Delta_f := f_1 - f_0$. Define the *sensitivity* of L as $\Delta_L := 2\Delta_\kappa + \Delta_f$.

We now present the *mixture upper confidence bound – continuum-armed bandit (Mixture-UCB-CAB) algorithm*. It has a parameter $\beta > 1$. It treats the online selection problem as multi-armed bandit with infinitely many arms similar to the continuum-armed bandit settings in [21, 31]. Each arm is a probability vector α . By pulling the arm α , we generate a sample from a randomly chosen model, where model i is chosen with probability α_i . Refer to Algorithm 1.

Similar to UCB, Mixture-UCB-CAB finds a lower confidence bound $\hat{L}(\alpha; \mathbf{x}^{(t)}) - (\epsilon^{(t)})^\top \alpha$ of the true loss $L(\alpha)$ at each round. To justify the expressions (6), (7), we prove that $\hat{L}(\alpha; \mathbf{x}^{(t)}) - (\epsilon^{(t)})^\top \alpha$ in (6) lower-bounds $L(\alpha)$ with probability at least $1 - t^{-\beta}$. The proof is given in Appendix A.1.

Theorem 1. *Fix a probability vector α .⁴ Suppose we have samples $x_{i,1}, \dots, x_{i,n_i}$ from the distribution P_i for $i = 1, \dots, m$, where n_i is the number of observed samples from model i . For $\delta > 0$,*

$$\mathbb{P}(\hat{L}(\alpha; \mathbf{x}) - L(\alpha) \geq \epsilon(\delta)^\top \alpha) \leq \delta, \quad \mathbb{P}(L(\alpha) - \hat{L}(\alpha; \mathbf{x}) \geq \epsilon(\delta)^\top \alpha) \leq \delta,$$

where $\epsilon(\delta) := (\Delta_L \sqrt{\frac{\log(1/\delta)}{2n_i}} + \frac{\Delta_\kappa}{n_i})_{i \in [m]}$.

⁴Theorem 1 holds for a fixed α . A worst-case bound that simultaneously holds for every α is in Lemma 1.

Algorithm 1 Mixture-UCB-CAB

- 1: **Input:** m generative arms, number of rounds T
- 2: **Output:** Gathered samples $\mathbf{x}^{(T)}$
- 3: **for** $t \in \{0, \dots, m-1\}$ **do**
- 4: Pull arm $t+1$ at time $t+1$ to obtain sample $x_{t+1,1} \sim P_{t+1}$. Set $n_{t+1}^{(m)} = 1$.
- 5: **end for**
- 6: **for** $t \in \{m, \dots, T-1\}$ **do**
- 7: Compute an estimate of the optimal mixture distribution via the convex quadratic program:

$$\boldsymbol{\alpha}^{(t)} := \operatorname{argmin}_{\boldsymbol{\alpha}} (\hat{L}(\boldsymbol{\alpha}; \mathbf{x}^{(t)}) - (\boldsymbol{\epsilon}^{(t)})^\top \boldsymbol{\alpha}), \quad (6)$$

where the minimization is over probability vectors $\boldsymbol{\alpha}$, and $\boldsymbol{\epsilon}^{(t)} \in \mathbb{R}^m$ is defined as

$$\epsilon_i^{(t)} := \Delta_L \sqrt{(\beta \log t) / (2n_i^{(t)})} + \Delta_\kappa / n_i^{(t)}. \quad (7)$$

- 8: Generate the arm index $b^{(t+1)} \in [m]$ at random with $\mathbb{P}(b^{(t+1)} = i) = \alpha_i^{(t)}$.
 - 9: Pull arm $b = b^{(t+1)}$ at time $t+1$ to obtain a new sample $x_{b, n_b^{(t)}+1} \sim P_b$. Set $n_b^{(t+1)} = n_b^{(t)} + 1$ and $n_j^{(t+1)} = n_j^{(t)}$ for $j \neq b$.³
 - 10: **end for** **return** samples $\mathbf{x}^{(T)}$
-

We now prove that Mixture-UCB-CAB gives an expected loss $\mathbb{E}[L(\hat{P}^{(T)})]$ that converges to the optimal loss $\min_{\boldsymbol{\alpha}} L(\boldsymbol{\alpha})$ by bounding their gap. This means that Mixture-UCB-CAB is a zero-regret strategy by treating $\mathbb{E}[L(\hat{P}^{(T)})] - \min_{\boldsymbol{\alpha}} L(\boldsymbol{\alpha})$ as the average regret per round.⁵ The proof is given in Appendix A.2.

Theorem 2. *Suppose $m \geq 2$, $\beta \geq 4$. Consider bounded quadratic loss function (4) with κ being positive semidefinite. Let $\hat{P}^{(T)}$ be the empirical distribution of the first $T \geq 2$ samples $\mathbf{x}^{(T)}$ given by Mixture-UCB-CAB. Then the gap between the expected loss and the optimal loss is bounded by*

$$\mathbb{E}[L(\hat{P}^{(T)})] - \min_{\boldsymbol{\alpha}} L(\boldsymbol{\alpha}) \leq 4\Delta_L \sqrt{\frac{\beta m \log T}{T}}.$$

When $\kappa(x, x') = 0$, Mixture-UCB-CAB reduces to the conventional UCB, and Theorem 2 coincides with the $O(\sqrt{(m \log T)/T})$ distribution-free bound on the regret per round of conventional UCB [20]. Since there is a $\Omega(\sqrt{m/T})$ minimax lower bound on the regret per round even for conventional multi-armed bandit without the quadratic kernel term [20, Theorem 3.4], Theorem 2 is tight up to a logarithmic factor.

The main difference between Mixture-UCB-CAB and conventional UCB is that we choose a mixture of arms in (6) given by the probability vector $\boldsymbol{\alpha}$, instead of a single arm. A more straightforward application of UCB would be to simply find the single arm that minimizes the lower bound in (6), i.e., we restrict $\boldsymbol{\alpha} = \mathbf{e}_i$ for some $i \in [m]$, where \mathbf{e}_i is the i -th basis vector, and minimize (6) over i instead. We call this *Vanilla-UCB*. Vanilla-UCB fails to take into account the possibility that a mixture may give a smaller loss than every single arm. In the long run, Vanilla-UCB converges to pulling the best single arm instead of the optimal mixture. Vanilla-UCB will be used as a baseline to be compared with Mixture-UCB-CAB, and another new algorithm presented in the next section.

Mixture-UCB-CAB can be extended to the Sparse-Mixture-UCB-CAB algorithm which eventually select only a small number of models. This can be useful if there is a subscription cost for each model. Refer to

⁵To justify calling $R := \mathbb{E}[L(\hat{P}^{(T)})] - \min_{\boldsymbol{\alpha}} L(\boldsymbol{\alpha})$ the average regret per round, note that when $\kappa(x, x') = 0$ and $f(x) = -r(x)$ where $r(x)$ is the reward of the sample x , i.e., the loss $L(P) = \mathbb{E}_{X \sim P}[f(X)]$ is linear, $T(\mathbb{E}[L(\hat{P}^{(T)})] - \min_{\boldsymbol{\alpha}} L(\boldsymbol{\alpha})) = T \max_{i \in [m]} \mathbb{E}_{X \sim P_i}[r(X)] - \mathbb{E}[\sum_{t=1}^T r(x^{(t)})]$ indeed reduces to the conventional notion of regret. So R can be regarded as the quadratic generalization of regret.

Algorithm 2 Mixture-UCB-OGD

- 1: **Input:** m generative arms, number of rounds T
- 2: **Output:** Gathered samples $\mathbf{x}^{(T)}$
- 3: **for** $t \in \{0, \dots, m-1\}$ **do**
- 4: Pull arm $t+1$ at time $t+1$ to obtain sample $x_{t+1,1} \sim P_{t+1}$
- 5: **end for**
- 6: **for** $t \in \{m, \dots, T-1\}$ **do**
- 7: Compute the gradient

$$\mathbf{h}^{(t)} := \nabla_{\alpha} \left(\hat{L}(\alpha; \mathbf{x}^{(t)}) - (\boldsymbol{\epsilon}^{(t)})^{\top} \alpha \right) \Big|_{\alpha = \mathbf{n}^{(t)}/t} = \frac{2}{t} \hat{\mathbf{K}}(\mathbf{x}^{(t)}) \mathbf{n}^{(t)} + \hat{\mathbf{f}}(\mathbf{x}^{(t)}) - \boldsymbol{\epsilon}^{(t)}, \quad (8)$$

where $\mathbf{n}^{(t)} := (n_i^{(t)})_{i \in [m]} \in \mathbb{R}^m$, and $\boldsymbol{\epsilon}^{(t)}$ is defined as in Mixture-UCB-CAB

- 8: Pull arm $b = b^{(t+1)} := \operatorname{argmin}_i h_i^{(t)}$ at time $t+1$ to obtain a new sample $x_{b, n_b^{(t)}+1} \sim P_b$.
 - 9: **end for** return samples $\mathbf{x}^{(T)}$
-

Appendix B for discussions.

5.2 Mixture Upper Confidence Bound – Online Gradient Descent

We present an alternative to Mixture-UCB-CAB, called the *mixture upper confidence bound – online gradient descent (Mixture-UCB-OGD) algorithm*, inspired by the online gradient descent algorithm [32]. It also has a parameter $\beta > 1$. Refer to Algorithm 2.

Mixture-UCB-CAB and Mixture-UCB-OGD can both be regarded as generalizations of the original UCB algorithm, in the sense that they reduce to UCB when $\kappa(x, x') = 0$. If we remove the $\frac{2}{t} \hat{\mathbf{K}}(\mathbf{x}) \mathbf{n}^{(t)}$ term in (8), then Mixture-UCB-OGD becomes the same as UCB.

Both Mixture-UCB-CAB and Mixture-UCB-OGD attempt to make the “proportion vector” $\mathbf{n}^{(t)}/t$ (note that $n_i^{(t)}/t$ is the proportion of samples from model i) approach the optimal mixture α^* that minimizes $L(\alpha)$, but they do so in different manners. Mixture-UCB-CAB first computes the estimate $\alpha^{(t)}$ after time t , then approaches $\alpha^{(t)}$ by pulling an arm randomly chosen from the distribution $\alpha^{(t)}$. Mixture-UCB-OGD estimates the gradient $\mathbf{h}^{(t)}$ of the loss function at the current proportion vector $\mathbf{n}^{(t)}/t$, and pulls an arm that results in the steepest descent of the loss.

An advantage of Mixture-UCB-OGD is that the computation of gradient (8) is significantly faster than the quadratic program (6) in Mixture-UCB-CAB. The running time complexity of Mixture-UCB-OGD is $O(T^2 + Tm^2)$.⁶ Nevertheless, a regret bound for Mixture-UCB-OGD similar to Theorem 2 seems to be difficult to derive, and is left for future research.

6 Numerical Results

We experiment on various scenarios to showcase the performance of our proposed algorithms. The experiments involve the following algorithms:

- **Mixture Oracle.** In the mixture oracle algorithm (Section 5), an oracle tells us the optimal mixture α^* in advance, and we pull arms randomly according to this distribution. The optimal mixture is calculated

⁵We may also consider the scenario where each pull gives a batch of l samples instead of only one sample. In this case, we will have $x_{b, m_b^{(t-1)}+1}, \dots, x_{b, n_b^{(t-1)}+l} \sim P_b$ and $n_b^{(t)} = n_b^{(t-1)} + l$.

⁶To update $\hat{\mathbf{K}}(\mathbf{x}^{(t)})$ after a new sample x' is obtained, we only need to compute $\kappa(x, x')$ for each existing sample x , and add their contributions to the corresponding entries in $\hat{\mathbf{K}}(\mathbf{x}^{(t)})$, requiring a computational time that is linear with the number of existing samples.

by solving the quadratic optimization in Section 4 on a large number of samples for each arm. The number of chosen samples varies based on the experiments. This is an unrealistic setting that only serves as a theoretical upper bound of the performance of any online algorithm. A realistic algorithm that performs close to the mixture oracle would be almost optimal.

- **One-Arm Oracle.** An oracle tells us the optimal single arm in advance, and we keep pulling this arm. This is an unrealistic setting. If our algorithms outperform the one-arm oracle, this will show that the advantage of pulling a mixture of arms (instead of a single arm) can be realistically achieved via online algorithms.
- **Vanilla-UCB.** A direct application of UCB mentioned near the end of Section 5.1. This serves as a baseline for the purpose of comparison.
- **Successive Halving.** The Success Halving algorithm [1, 2, 3] which serves as a second baseline for comparison.
- **Mixture-UCB-CAB.** The mixture upper confidence bound – continuum-armed bandit algorithm proposed in Section 5.1.
- **Mixture-UCB-OGD.** The mixture upper confidence bound – online gradient descent algorithm proposed in Section 5.2.

Experiments Setup. We use DINOv2-ViT-L/14 [33] for image feature extraction, as recommended by [34], and use RoBERTa [35] as text encoder. Detailed explanation of the setup for each experiment is presented in Section C.1.

6.1 Optimal Mixture for Diversity and Quality via KID

We conduct three experiments to evaluate our method using the Kernel Inception Distance (KID) metric. In the first experiment, we use five distinct generative models: LDM [36], StyleGAN-XL [37], Efficient-vdVAE [38], InsGen [39], and StyleNAT [40], all trained on the FFHQ dataset [41]. In the second experiment, we use generated images from four models⁷: StyleGAN [41], Projected GAN [42], iDDPM [43], and Unleashing Transformers [44], all trained on the LSUN-Bedroom dataset [45]. This experiment follows a similar setup to the first. In the final experiment, we employ the Truncation Method [41, 46] to generate diversity-controlled images centered on eight randomly selected points, using StyleGAN2-ADA [47], also trained on the FFHQ dataset. Figure 3 demonstrates that the mixture of generators achieves a better KID score compared to individual models. Additionally, the two Mixture-UCB algorithms consistently outperform the baselines.

6.2 Optimal Mixture for Diversity via RKE

We use the RKE Mode Count [7] as an evaluation metric to show the effect of mixing the models on the diversity and the advantage of our algorithms Mixture-UCB-CAB and Mixture-UCB-OGD. The score in the plots is the RKE Mode Count, written as RKE for brevity.

Synthetic Unconditional Generative Models We conduct two experiments on diversity-limited generative models. First, we use eight center points with a truncation value of 0.3 to generate images using StyleGAN2-ADA, trained on the FFHQ dataset. In the second experiment, we apply the same model, trained on the AFHQ Cat dataset [48], with a truncation value of 0.4. As shown in Figure 4, the mixture achieves a higher RKE score, and our algorithms consistently get a higher RKE value. The increase in diversity is visually depicted in Figures 8 and 9.

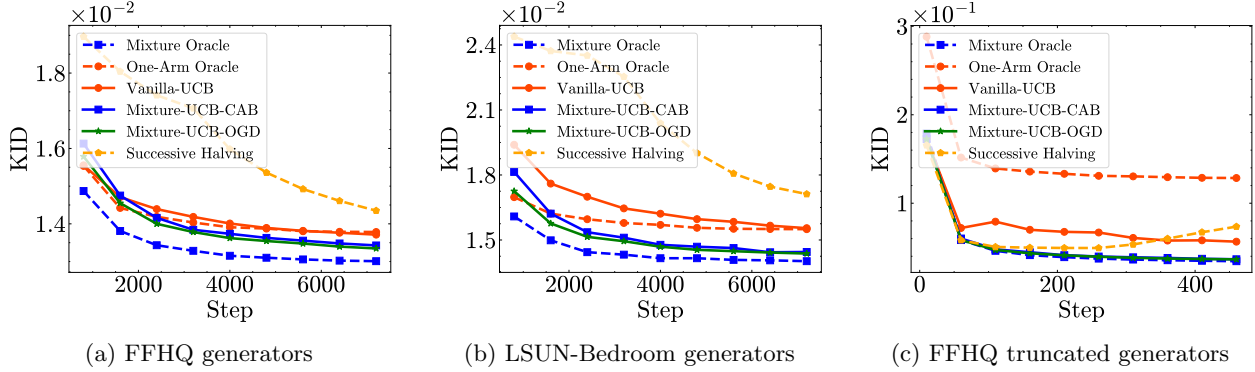


Figure 3: Performance comparison of online algorithms for the KID metric across FFHQ, LSUN-Bedroom, and FFHQ Truncated generators.

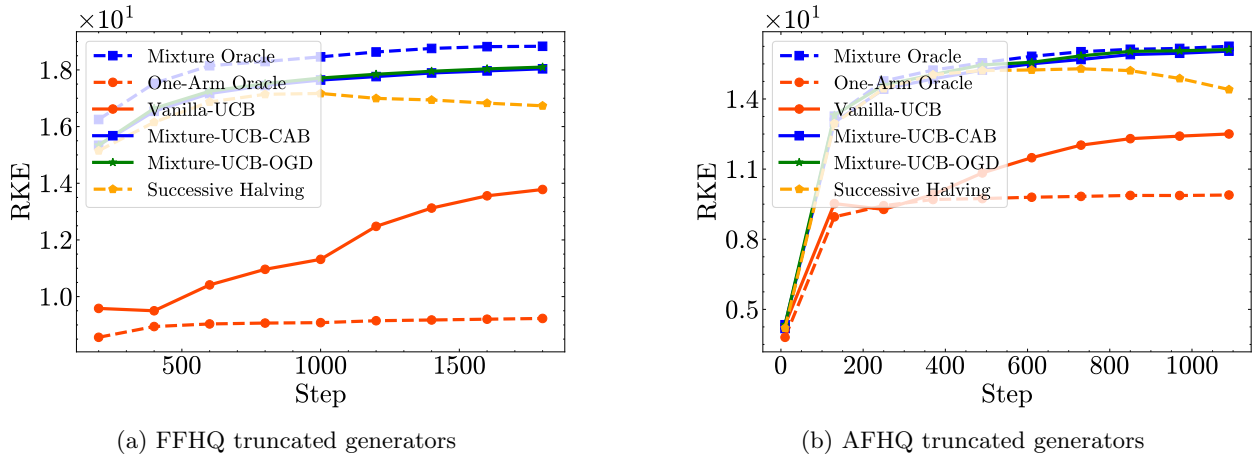


Figure 4: Performance comparison of online algorithms based on the RKE metric for Simulator Unconditional Generative Models.

Text to Image Generative Models Given that many text-to-image generative models are trained on different datasets, we expect a more pronounced increase in diversity when using a mixture of these models, compared to unconditional generative models trained on the same dataset, such as FFHQ.

We explore three scenarios to evaluate the performance of our algorithms. First, we simulate when models struggle to capture different styles. To address this, we use Stable Diffusion XL [49] with specific prompts to create three car image generators with distinct styles: realistic, surreal, and cartoon. In the second experiment, recognizing the importance of diversity in generative models for design tasks, we use four models—FLUX.1-Schnell [50], Kandinsky 3.0 [51], PixArt- α [52], and Stable Diffusion XL—to generate images of the object “Sofa”. In a similar manner, we generate red cartoonish bird images using Kandinsky 3.0, Stable Diffusion 3 [53], and PixArt- α . The increase in diversity is shown in Figure 1. The performance of our online algorithms and the comparison of samples generated by them with the baselines are shown in Figure 2. Finally, in the last experiment, we use Stable Diffusion XL to simulate models generating images of different dog breeds: Bulldog, German Shepherd, and Poodle, respectively. This illustrates the challenge of generating diverse object types with text-to-image models. Figure 5 illustrates the impact of using a mixture of models in the first and last experiments. The improvement in diversity is evident both visually

⁷FFHQ and LSUN-Bedroom datasets were downloaded from the dgm-eval repository [34] (licensed under MIT license): <https://github.com/layer6ai-labs/dgm-eval>.

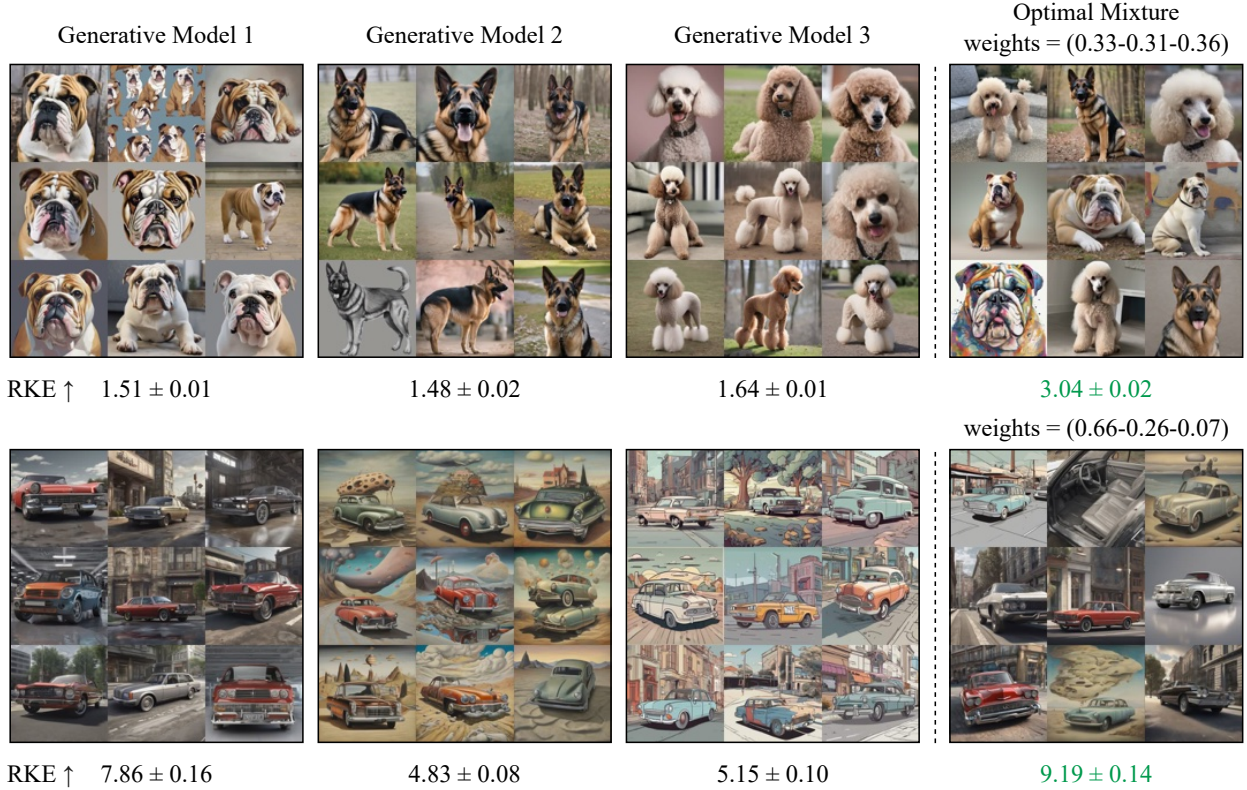


Figure 5: Visual comparison of the diversity across individual arms and the optimal mixture for Dog Breed Generators and Style-Specific Generators.

and quantitatively, as reflected in the RKE Scores. As shown in Figure 6, our online algorithms consistently outperform others in generating more diverse samples.

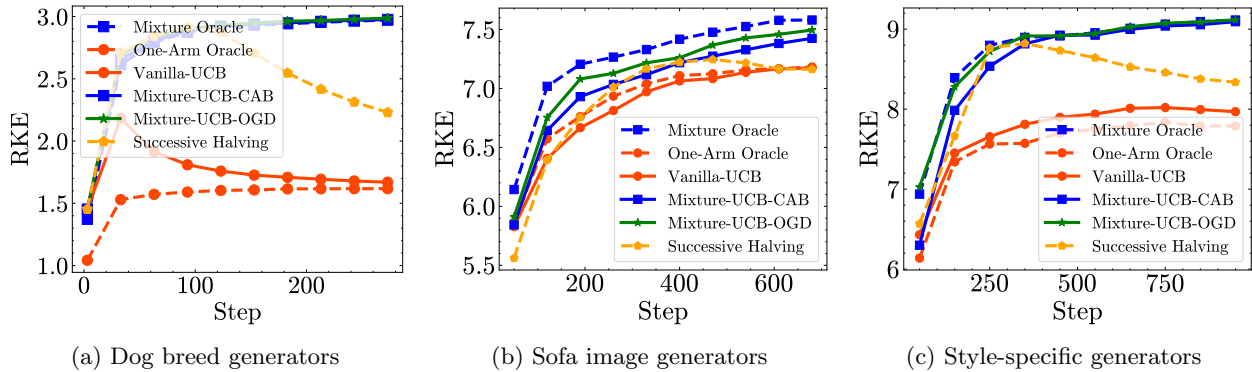


Figure 6: Performance comparison of online algorithms using the RKE metric for text-to-image generative models.

Text Generative Models We utilize the OpenLLMText dataset [54], which comprises 60,000 human texts rephrased paragraph by paragraph using the GPT2-XL [55], LLaMA-7B [56], and PaLM [57] models. To extract textual features, we employ the RoBERTa Text Encoder. As shown in Figure 11a in Section C.3, the

results demonstrate the advantage of our online algorithms, suggesting that our method applies not only to image generators, but also to text generators.

6.3 Optimal Mixture for Diversity and Quality via RKE and Precision/Density

Using RKE, we focus solely on the diversity of the models without accounting for their quality. To address this, we apply our methodology to both RKE and Precision [9], as well as RKE and Density [10]. We conduct experiments in which quality is a key consideration. We use four models: three are StyleGAN2-ADA models trained on the FFHQ dataset, each generating images with a truncation of 0.3 around randomly selected center points. The fourth model is StyleGAN2-ADA trained on CIFAR-10 [58]. The FFHQ dataset is used as the reference dataset, therefore, the model trained on CIFAR-10 acts as a low quality generator. Figures 7 and 12 demonstrate the ability of our algorithms to find optimal mixtures with a higher diversity/quality score.

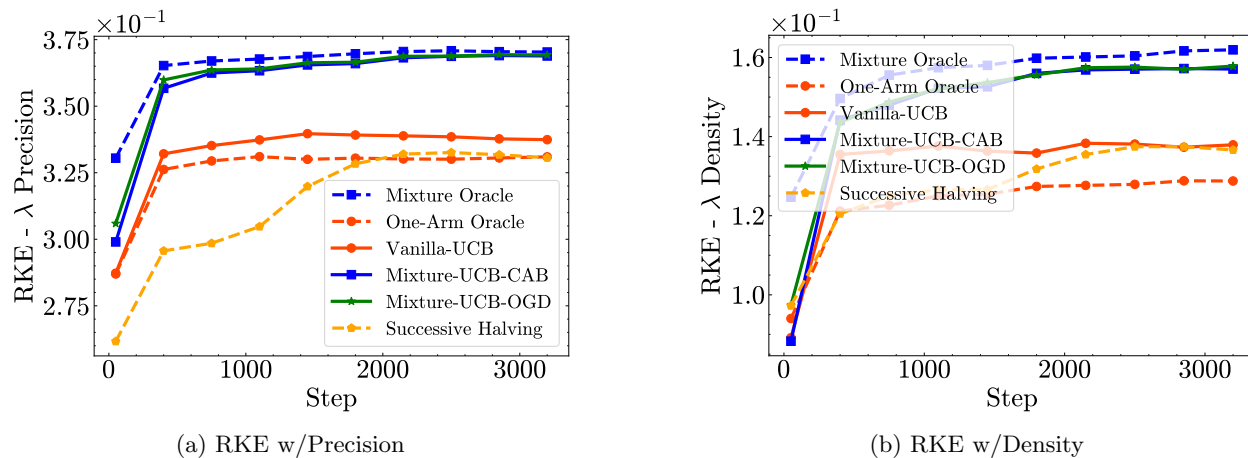


Figure 7: Performance comparison of online algorithms using the combination of RKE with Precision and RKE with Density metrics.

7 Conclusion

We studied the online selection from several generative models, where the online learner aims to generate samples with the best overall quality and diversity. While standard multi-armed bandit (MAB) algorithms aim to converge to one arm and select one generative model, we highlighted the fact that a mixture of generative models could achieve a higher score compared to each individual model. We proposed the Mixture-UCB-CAB and Mixture-UCB-OGD online learning algorithms to find the optimal mixture. Our experiments suggest the usefulness of the algorithm in improving the performance scores over individual arms. Extending the algorithm to conditional and text-based generative models is a topic for future exploration. In addition, the application of the algorithm to other data domains, including text, audio, and video, is an interesting future direction.

References

- [1] Zohar Karnin, Tomer Koren, and Oren Somekh. Almost optimal exploration in multi-armed bandits. In *International conference on machine learning*, pages 1238–1246. PMLR, 2013.

- [2] Kevin Jamieson and Ameet Talwalkar. Non-stochastic best arm identification and hyperparameter optimization. In *Artificial intelligence and statistics*, pages 240–248. PMLR, 2016.
- [3] Luming Chen and Sujit K Ghosh. Fast model selection and hyperparameter tuning for generative models. *Entropy*, 26(2):150, 2024.
- [4] Arthur Gretton, Karsten M Borgwardt, Malte J Rasch, Bernhard Schölkopf, and Alexander Smola. A kernel two-sample test. *The Journal of Machine Learning Research*, 13(1):723–773, 2012.
- [5] Xiaoyan Hu, Ho-fung Leung, and Farzan Farnia. An optimism-based approach to online evaluation of generative models. *arXiv preprint arXiv:2406.07451*, 2024.
- [6] Miłkołaj Bińkowski, Danica J Sutherland, Michael Arbel, and Arthur Gretton. Demystifying MMD GANs. In *International Conference on Learning Representations*, 2018.
- [7] Mohammad Jalali, Cheuk Ting Li, and Farzan Farnia. An information-theoretic evaluation of generative models in learning multi-modal distributions. *Advances in Neural Information Processing Systems*, 36, 2023.
- [8] Mehdi SM Sajjadi, Olivier Bachem, Mario Lucic, Olivier Bousquet, and Sylvain Gelly. Assessing generative models via precision and recall. *Advances in neural information processing systems*, 31, 2018.
- [9] Tuomas Kynkäänniemi, Tero Karras, Samuli Laine, Jaakko Lehtinen, and Timo Aila. *Improved precision and recall metric for assessing generative models*. Curran Associates Inc., Red Hook, NY, USA, 2019.
- [10] Muhammad Ferjad Naeem, Seong Joon Oh, Youngjung Uh, Yunjey Choi, and Jaejun Yoo. Reliable fidelity and diversity metrics for generative models. In *Proceedings of the 37th International Conference on Machine Learning*, ICML’20. JMLR.org, 2020.
- [11] Dan Friedman and Adji Bousso Dieng. The vendi score: A diversity evaluation metric for machine learning. *Transactions on Machine Learning Research*, 2023.
- [12] Azim Osmanov, Jingwei Zhang, Mohammad Jalali, Xuenan Cao, Andrej Bogdanov, and Farzan Farnia. Towards a scalable reference-free evaluation of generative models. In *The Thirty-eighth Annual Conference on Neural Information Processing Systems*, 2024.
- [13] Martin Arjovsky, Soumith Chintala, and Léon Bottou. Wasserstein generative adversarial networks. In Doina Precup and Yee Whye Teh, editors, *Proceedings of the 34th International Conference on Machine Learning*, volume 70 of *Proceedings of Machine Learning Research*, pages 214–223. PMLR, 06–11 Aug 2017.
- [14] Martin Heusel, Hubert Ramsauer, Thomas Unterthiner, Bernhard Nessler, and Sepp Hochreiter. Gans trained by a two time-scale update rule converge to a local nash equilibrium. In *Proceedings of the 31st International Conference on Neural Information Processing Systems*, NIPS’17, page 6629–6640, Red Hook, NY, USA, 2017. Curran Associates Inc.
- [15] Jingwei Zhang, Cheuk Ting Li, and Farzan Farnia. An interpretable evaluation of entropy-based novelty of generative models. *arXiv preprint arXiv:2402.17287*, 2024.
- [16] T.L Lai and Herbert Robbins. Asymptotically efficient adaptive allocation rules. *Advances in Applied Mathematics*, 6(1):4–22, 1985.
- [17] William R. Thompson. On the likelihood that one unknown probability exceeds another in view of the evidence of two samples. *Biometrika*, 25(3/4):285–294, 1933.
- [18] Rajeev Agrawal. Sample mean based index policies by $O(\log n)$ regret for the multi-armed bandit problem. *Advances in applied probability*, 27(4):1054–1078, 1995.

- [19] Peter Auer. Using confidence bounds for exploitation-exploration trade-offs. *J. Mach. Learn. Res.*, 3:397–422, March 2003.
- [20] Sébastien Bubeck and Cesa-Bianchi Nicolò. 2012.
- [21] Rajeev Agrawal. The continuum-armed bandit problem. *SIAM Journal on Control and Optimization*, 33(6):1926–1951, 1995.
- [22] Matthias Feurer and Frank Hutter. *Hyperparameter Optimization*, pages 3–33. Springer International Publishing, Cham, 2019.
- [23] Lisha Li, Kevin Jamieson, Giulia DeSalvo, Afshin Rostamizadeh, and Ameet Talwalkar. Hyperband: A novel bandit-based approach to hyperparameter optimization. *Journal of Machine Learning Research*, 18(185):1–52, 2018.
- [24] Shashank Singh. Continuum-armed bandits: A function space perspective. In Arindam Banerjee and Kenji Fukumizu, editors, *Proceedings of The 24th International Conference on Artificial Intelligence and Statistics*, volume 130 of *Proceedings of Machine Learning Research*, pages 2620–2628. PMLR, 13–15 Apr 2021.
- [25] Robert Kleinberg. Nearly tight bounds for the continuum-armed bandit problem. In *Proceedings of the 17th International Conference on Neural Information Processing Systems*, NIPS’04, page 697–704, Cambridge, MA, USA, 2004. MIT Press.
- [26] Robert Kleinberg, Aleksandrs Slivkins, and Eli Upfal. Bandits and experts in metric spaces. *J. ACM*, 66(4), May 2019.
- [27] Sébastien Bubeck, Gilles Stoltz, Csaba Szepesvári, and Rémi Munos. Online optimization in x-armed bandits. In D. Koller, D. Schuurmans, Y. Bengio, and L. Bottou, editors, *Advances in Neural Information Processing Systems*, volume 21. Curran Associates, Inc., 2008.
- [28] Nir Weinberger and Michal Yemini. Multi-armed bandits with self-information rewards. *IEEE Transactions on Information Theory*, 69(11):7160–7184, 2023.
- [29] Xiaoyan Hu, Ho-fung Leung, and Farzan Farnia. An online learning approach to prompt-based selection of generative models. *arXiv preprint arXiv:2410.13287*, 2024.
- [30] Christian Szegedy, Vincent Vanhoucke, Sergey Ioffe, Jon Shlens, and Zbigniew Wojna. Rethinking the inception architecture for computer vision. In *Proceedings of the IEEE conference on computer vision and pattern recognition*, pages 2818–2826, 2016.
- [31] Shiyin Lu, Guanghui Wang, Yao Hu, and Lijun Zhang. Optimal algorithms for lipschitz bandits with heavy-tailed rewards. In *International Conference on Machine Learning*, pages 4154–4163. PMLR, 2019.
- [32] Shai Shalev-Shwartz et al. Online learning and online convex optimization. *Foundations and Trends® in Machine Learning*, 4(2):107–194, 2012.
- [33] Maxime Oquab, Timothée Darcet, Théo Moutakanni, Huy V. Vo, Marc Szafraniec, Vasil Khalidov, Pierre Fernandez, Daniel HAZIZA, Francisco Massa, Alaaeldin El-Nouby, Mido Assran, Nicolas Ballas, Wojciech Galuba, Russell Howes, Po-Yao Huang, Shang-Wen Li, Ishan Misra, Michael Rabbat, Vasu Sharma, Gabriel Synnaeve, Hu Xu, Herve Jegou, Julien Mairal, Patrick Labatut, Armand Joulin, and Piotr Bojanowski. DINOv2: Learning robust visual features without supervision. *Transactions on Machine Learning Research*, 2024. Featured Certification.
- [34] George Stein, Jesse Cresswell, Rasa Hosseinzadeh, Yi Sui, Brendan Ross, Valentin Vilecroze, Zhaoyan Liu, Anthony L Caterini, Eric Taylor, and Gabriel Loaiza-Ganem. Exposing flaws of generative model evaluation metrics and their unfair treatment of diffusion models. In *Advances in Neural Information Processing Systems*, volume 36, 2023.

- [35] Yinhan Liu, Myle Ott, Naman Goyal, Jingfei Du, Mandar Joshi, Danqi Chen, Omer Levy, Mike Lewis, Luke Zettlemoyer, and Veselin Stoyanov. Roberta: A robustly optimized bert pretraining approach, 2019.
- [36] Robin Rombach, A. Blattmann, Dominik Lorenz, Patrick Esser, and Björn Ommer. High-resolution image synthesis with latent diffusion models. *2022 IEEE/CVF Conference on Computer Vision and Pattern Recognition (CVPR)*, pages 10674–10685, 2021.
- [37] Axel Sauer, Katja Schwarz, and Andreas Geiger. Stylegan-xl: Scaling stylegan to large diverse datasets. In *ACM SIGGRAPH 2022 Conference Proceedings, SIGGRAPH '22*, New York, NY, USA, 2022. Association for Computing Machinery.
- [38] Louay Hazami, Rayhane Mama, and Ragavan Thurairatnam. Efficient-ldvae: Less is more, 2022.
- [39] Ceyuan Yang, Yujun Shen, Yinghao Xu, and Bolei Zhou. Data-efficient instance generation from instance discrimination. In M. Ranzato, A. Beygelzimer, Y. Dauphin, P.S. Liang, and J. Wortman Vaughan, editors, *Advances in Neural Information Processing Systems*, volume 34, pages 9378–9390. Curran Associates, Inc., 2021.
- [40] Steven Walton, Ali Hassani, Xingqian Xu, Zhangyang Wang, and Humphrey Shi. Stylenat: Giving each head a new perspective, 2023.
- [41] Tero Karras, Samuli Laine, and Timo Aila. A style-based generator architecture for generative adversarial networks. In *2019 IEEE/CVF Conference on Computer Vision and Pattern Recognition (CVPR)*, pages 4396–4405, 2019.
- [42] Axel Sauer, Kashyap Chitta, Jens Müller, and Andreas Geiger. Projected gans converge faster. In M. Ranzato, A. Beygelzimer, Y. Dauphin, P.S. Liang, and J. Wortman Vaughan, editors, *Advances in Neural Information Processing Systems*, volume 34, pages 17480–17492. Curran Associates, Inc., 2021.
- [43] Alex Nichol and Prafulla Dhariwal. Improved denoising diffusion probabilistic models, 2021.
- [44] Sam Bond-Taylor, Peter Hesse, Hiroshi Sasaki, Toby P. Breckon, and Chris G. Willcocks. Unleashing transformers: Parallel token prediction with discrete absorbing diffusion for fast high-resolution image generation from vector-quantized codes, 2021.
- [45] Fisher Yu, Ari Seff, Yinda Zhang, Shuran Song, Thomas Funkhouser, and Jianxiong Xiao. Lsun: Construction of a large-scale image dataset using deep learning with humans in the loop, 2016.
- [46] Marco Marchesi. Megapixel size image creation using generative adversarial networks, 2017.
- [47] Tero Karras, Miika Aittala, Janne Hellsten, Samuli Laine, Jaakko Lehtinen, and Timo Aila. Training generative adversarial networks with limited data. In *Proceedings of the 34th International Conference on Neural Information Processing Systems, NIPS '20*, Red Hook, NY, USA, 2020. Curran Associates Inc.
- [48] Yunjey Choi, Youngjung Uh, Jaejun Yoo, and Jung-Woo Ha. Stargan v2: Diverse image synthesis for multiple domains. In *Proceedings of the IEEE Conference on Computer Vision and Pattern Recognition*, 2020.
- [49] Dustin Podell, Zion English, Kyle Lacey, Andreas Blattmann, Tim Dockhorn, Jonas Müller, Joe Penna, and Robin Rombach. SDXL: Improving latent diffusion models for high-resolution image synthesis. In *The Twelfth International Conference on Learning Representations*, 2024.
- [50] Black Forest Lab. Flux: A diffusion-based text-to-image (t2i) model. <https://github.com/blackforestlab/flux>, 2024. Accessed: 2024-09.

- [51] Vladimir Arkhipkin, Viacheslav Vasilev, Andrei Filatov, Igor Pavlov, Julia Agafonova, Nikolai Gerashenko, Anna Averchenkova, Evelina Mironova, Anton Bukashkin, Konstantin Kulikov, Andrey Kuznetsov, and Denis Dimitrov. Kandinsky 3: Text-to-image synthesis for multifunctional generative framework, 2024.
- [52] Junsong Chen, Jincheng Yu, Chongjian Ge, Lewei Yao, Enze Xie, Yue Wu, Zhongdao Wang, James Kwok, Ping Luo, Huchuan Lu, and Zhenguo Li. Pixart- α : Fast training of diffusion transformer for photorealistic text-to-image synthesis, 2023.
- [53] Patrick Esser, Sumith Kulal, Andreas Blattmann, Rahim Entezari, Jonas Müller, Harry Saini, Yam Levi, Dominik Lorenz, Axel Sauer, Frederic Boesel, Dustin Podell, Tim Dockhorn, Zion English, Kyle Lacey, Alex Goodwin, Yannik Marek, and Robin Rombach. Scaling rectified flow transformers for high-resolution image synthesis, 2024.
- [54] Yutian Chen, Hao Kang, Yiyan Zhai, Liangze Li, Rita Singh, and Bhiksha Raj. Openllmtext dataset, 2023.
- [55] Alec Radford, Jeff Wu, Rewon Child, David Luan, Dario Amodei, and Ilya Sutskever. Language models are unsupervised multitask learners. 2019.
- [56] Hugo Touvron, Thibaut Lavril, Gautier Izacard, Xavier Martinet, Marie-Anne Lachaux, Timothée Lacroix, Baptiste Rozière, Naman Goyal, Eric Hambro, Faisal Azhar, Aurelien Rodriguez, Armand Joulin, Edouard Grave, and Guillaume Lample. Llama: Open and efficient foundation language models, 2023.
- [57] Aakanksha Chowdhery, Sharan Narang, Jacob Devlin, Maarten Bosma, Gaurav Mishra, Adam Roberts, Paul Barham, Hyung Won Chung, Charles Sutton, Sebastian Gehrmann, Parker Schuh, Kensen Shi, Sasha Tsvyashchenko, Joshua Maynez, Abhishek Rao, Parker Barnes, Yi Tay, Noam Shazeer, Vinodkumar Prabhakaran, Emily Reif, Nan Du, Ben Hutchinson, Reiner Pope, James Bradbury, Jacob Austin, Michael Isard, Guy Gur-Ari, Pengcheng Yin, Toju Duke, Anselm Levskaya, Sanjay Ghemawat, Sunipa Dev, Henryk Michalewski, Xavier Garcia, Vedant Misra, Kevin Robinson, Liam Fedus, Denny Zhou, Daphne Ippolito, David Luan, Hyeontaek Lim, Barret Zoph, Alexander Spiridonov, Ryan Sepassi, David Dohan, Shivani Agrawal, Mark Omernick, Andrew M. Dai, Thanumalayan Sankaranarayanan Pillai, Marie Pellat, Aitor Lewkowycz, Erica Moreira, Rewon Child, Oleksandr Polozov, Katherine Lee, Zongwei Zhou, Xuezhi Wang, Brennan Saeta, Mark Diaz, Orhan Firat, Michele Catasta, Jason Wei, Kathy Meier-Hellstern, Douglas Eck, Jeff Dean, Slav Petrov, and Noah Fiedel. Palm: scaling language modeling with pathways. *J. Mach. Learn. Res.*, 24(1), March 2024.
- [58] Alex Krizhevsky and Geoffrey Hinton. Learning multiple layers of features from tiny images. Technical Report 0, University of Toronto, Toronto, Ontario, 2009.
- [59] OpenAI. Gpt-4 technical overview. <https://openai.com/research/gpt-4>, 2024. Accessed: 2024-10.

A Proofs

A.1 Proof of Theorem 1

Consider any $\tilde{x}_{i,a} \in \mathcal{X}$. Let $\tilde{\mathbf{x}}$ be the samples which are identical to \mathbf{x} except that one entry $x_{i,a}$ is changed to $\tilde{x}_{i,a}$. We have

$$\begin{aligned}
& \left| \hat{L}(\boldsymbol{\alpha}; \tilde{\mathbf{x}}) - \hat{L}(\boldsymbol{\alpha}; \mathbf{x}) \right| \\
&= \left| \frac{\alpha_i}{n_i} (f(\tilde{x}_{i,a}) - f(x_{i,a})) + 2 \sum_{(j,b) \neq (i,a)} \frac{\alpha_i \alpha_j}{n_i n_j} (\kappa(\tilde{x}_{i,a}, x_{j,b}) - \kappa(x_{i,a}, x_{j,b})) \right. \\
&\quad \left. + \frac{\alpha_i^2}{n_i^2} (\kappa(\tilde{x}_{i,a}, \tilde{x}_{i,a}) - \kappa(x_{i,a}, x_{i,a})) \right| \\
&\leq \frac{\alpha_i}{n_i} \Delta_f + 2 \sum_{(j,b) \neq (i,a)} \frac{\alpha_i \alpha_j}{n_i n_j} \Delta_\kappa + \frac{\alpha_i^2}{n_i^2} \Delta_\kappa \\
&\leq \frac{\alpha_i}{n_i} (\Delta_f + 2\Delta_\kappa) \\
&= \frac{\alpha_i}{n_i} \Delta_L.
\end{aligned}$$

By McDiarmid's inequality,

$$\begin{aligned}
\mathbb{P} \left(\hat{L}(\boldsymbol{\alpha}; \mathbf{x}) - \mathbb{E}[\hat{L}(\boldsymbol{\alpha}; \mathbf{x})] \geq \epsilon \right) &\leq \exp \left(-\frac{2\epsilon^2}{\sum_{i=1}^m \sum_{a=1}^{n_i} \left(\frac{\alpha_i}{n_i} \Delta_L \right)^2} \right) \\
&= \exp \left(-\frac{2\epsilon^2}{\Delta_L^2 \sum_{i=1}^m \alpha_i^2 / n_i} \right).
\end{aligned}$$

Note that

$$\begin{aligned}
& \left| L(\boldsymbol{\alpha}) - \mathbb{E}[\hat{L}(\boldsymbol{\alpha}; \mathbf{x})] \right| \\
&= \left| \mathbb{E}_{X, X' \stackrel{\text{iid}}{\sim} P} [\kappa(X, X')] - \mathbb{E} \left[\sum_{(i,j) \in [m]^2} \frac{\alpha_i \alpha_j}{n_i n_j} \sum_{a=1}^{n_i} \sum_{b=1}^{n_j} \kappa(x_{i,a}, x_{j,b}) \right] \right| \\
&= \left| \sum_{i=1}^m \frac{\alpha_i^2}{n_i^2} \sum_{a=1}^{n_i} \left(\mathbb{E}_{X, X' \stackrel{\text{iid}}{\sim} P} [\kappa(X, X')] - \mathbb{E}[\kappa(x_{i,a}, x_{i,a})] \right) \right| \\
&\leq \sum_{i=1}^m \frac{\alpha_i^2}{n_i} \Delta_\kappa.
\end{aligned}$$

Hence, for $\delta > 0$,

$$\mathbb{P} \left(\hat{L}(\boldsymbol{\alpha}; \mathbf{x}) - L(\boldsymbol{\alpha}) \geq \Delta_L \sqrt{\frac{\log(1/\delta)}{2} \sum_{i=1}^m \frac{\alpha_i^2}{n_i}} + \Delta_\kappa \sum_{i=1}^m \frac{\alpha_i^2}{n_i} \right) \leq \delta.$$

The result follows from

$$\begin{aligned}
& \Delta_L \sqrt{\frac{\log(1/\delta)}{2} \sum_{i=1}^m \frac{\alpha_i^2}{n_i}} + \Delta_\kappa \sum_{i=1}^m \frac{\alpha_i^2}{n_i} \\
&\leq \Delta_L \sum_{i=1}^m \sqrt{\frac{\log(1/\delta)}{2} \frac{\alpha_i^2}{n_i}} + \Delta_\kappa \sum_{i=1}^m \frac{\alpha_i}{n_i}
\end{aligned}$$

$$= \sum_{i=1}^m \left(\Delta_L \sqrt{\frac{\log(1/\delta)}{2n_i}} + \frac{\Delta_\kappa}{n_i} \right) \alpha_i.$$

The other direction of the inequality is similar.

A.2 Proof of Theorem 2

Before we prove Theorem 2, we first prove a worst case concentration bound.

Lemma 1. *Let $T \geq 2$, and $x_{i,1}, x_{i,2}, \dots \stackrel{\text{iid}}{\sim} P_i$ for $i \in [m]$. Let $\Delta_L := 2\Delta_\kappa + \Delta_f$. For $n_1, \dots, n_m \in [T]$, let $\mathbf{x}^{(n_i)_i} := (x_{i,a})_{i \in [m], a \in [n_i]}$. Fix any $\delta > 0$. With probability at least $1 - \delta$, we have*

$$\begin{aligned} & L(\boldsymbol{\alpha}) - \hat{L}(\boldsymbol{\alpha}; \mathbf{x}^{(n_i)_i}) \\ & \leq \sum_{i=1}^m \left(\Delta_L \sqrt{\frac{1}{2n_i} \log \frac{m^2 T^2}{2\delta}} + \frac{\Delta_\kappa}{n_i} \right) \alpha_i. \end{aligned}$$

for every $n_1, \dots, n_m \in [T]$ and probability vector $\boldsymbol{\alpha}$. The same holds for $\hat{L}(\boldsymbol{\alpha}; \mathbf{x}^{(n_i)_i}) - L(\boldsymbol{\alpha})$ instead of $L(\boldsymbol{\alpha}) - \hat{L}(\boldsymbol{\alpha}; \mathbf{x}^{(n_i)_i})$.

Proof: Fix any $n_1, \dots, n_m \in [T]$, and write $\mathbf{x} = \mathbf{x}^{(n_i)_i}$. We have

$$\begin{aligned} & L(\boldsymbol{\alpha}) - \hat{L}(\boldsymbol{\alpha}; \mathbf{x}) \\ & = \sum_{i,j} \alpha_i \alpha_j \left(\frac{\mathbf{f}_i + \mathbf{f}_j}{2} + \mathbf{K}_{i,j} - \frac{\hat{\mathbf{f}}_i(\mathbf{x}) + \hat{\mathbf{f}}_j(\mathbf{x})}{2} - \hat{\mathbf{K}}_{i,j}(\mathbf{x}) \right). \end{aligned}$$

For $i = j$, applying Theorem 1 on $\boldsymbol{\alpha}$ being the i -th basis vector,

$$\mathbb{P} \left(\mathbf{f}_i + \mathbf{K}_{i,i} - \hat{\mathbf{f}}_i(\mathbf{x}) - \hat{\mathbf{K}}_{i,i}(\mathbf{x}) \geq \Delta_L \sqrt{\frac{\log(1/\delta)}{2n_i}} + \frac{\Delta_\kappa}{n_i} \right) \leq \delta. \quad (9)$$

For $i \neq j$, we will use similar arguments as Theorem 1. Let $\tilde{\mathbf{x}}$ be the samples which are identical to \mathbf{x} except that one entry $x_{i,a}$ of the i -th arm is changed to $\tilde{x}_{i,a}$. We have

$$\begin{aligned} & \left| \frac{\hat{\mathbf{f}}_i(\tilde{\mathbf{x}}) + \hat{\mathbf{f}}_j(\tilde{\mathbf{x}})}{2} + \hat{\mathbf{K}}_{i,j}(\tilde{\mathbf{x}}) - \frac{\hat{\mathbf{f}}_i(\mathbf{x}) + \hat{\mathbf{f}}_j(\mathbf{x})}{2} - \hat{\mathbf{K}}_{i,j}(\mathbf{x}) \right| \\ & = \left| \frac{1}{2n_i} (f(\tilde{x}_{i,a}) - f(x_{i,a})) + \frac{1}{n_i n_j} \sum_{b=1}^{n_j} (\kappa(\tilde{x}_{i,a}, x_{j,b}) - \kappa(x_{i,a}, x_{j,b})) \right| \\ & \leq \frac{\Delta_f}{2n_i} + \frac{\Delta_\kappa}{n_i} \\ & = \frac{\Delta_L}{2n_i}. \end{aligned}$$

Note that $\mathbb{E} \left[\frac{\hat{\mathbf{f}}_i(\mathbf{x}) + \hat{\mathbf{f}}_j(\mathbf{x})}{2} + \hat{\mathbf{K}}_{i,j}(\mathbf{x}) \right] = \frac{\mathbf{f}_i + \mathbf{f}_j}{2} + \mathbf{K}_{i,j}$. By McDiarmid's inequality,

$$\mathbb{P} \left(\frac{\mathbf{f}_i + \mathbf{f}_j}{2} + \mathbf{K}_{i,j} - \frac{\hat{\mathbf{f}}_i(\mathbf{x}) + \hat{\mathbf{f}}_j(\mathbf{x})}{2} - \hat{\mathbf{K}}_{i,j}(\mathbf{x}) \geq \epsilon \right)$$

$$\begin{aligned}
&\leq \exp\left(-\frac{2\epsilon^2}{n_i\left(\frac{\Delta_L}{2n_i}\right)^2 + n_j\left(\frac{\Delta_L}{2n_j}\right)^2}\right) \\
&= \exp\left(-\frac{8\epsilon^2}{\Delta_L^2(n_i^{-1} + n_j^{-1})}\right).
\end{aligned}$$

Hence,

$$\mathbb{P}\left(\frac{\mathbf{f}_i + \mathbf{f}_j}{2} + \mathbf{K}_{i,j} - \frac{\hat{\mathbf{f}}_i(\mathbf{x}) + \hat{\mathbf{f}}_j(\mathbf{x})}{2} - \hat{\mathbf{K}}_{i,j}(\mathbf{x}) \geq \Delta_L \sqrt{\frac{\log(1/\delta)}{8}(n_i^{-1} + n_j^{-1})}\right) \leq \delta. \quad (10)$$

Note that the event in (9) does not depend on $n_{i'}$ for $i' \neq i$, and the event in (10) does not depend on $n_{i'}$ for $i' \notin \{i, j\}$. By union bound, all the events in (9) and (10) do not hold for all $i \leq j$ and $n_1, \dots, n_m \in [T]$ with probability at least

$$1 - mT\delta - \frac{m(m-1)}{2}T^2\delta \geq 1 - \frac{m^2}{2}T^2\delta.$$

If these events do not hold, then

$$\begin{aligned}
&L(\boldsymbol{\alpha}) - \hat{L}(\boldsymbol{\alpha}; \mathbf{x}) \\
&= \sum_{i,j} \alpha_i \alpha_j \left(\frac{\mathbf{f}_i + \mathbf{f}_j}{2} + \mathbf{K}_{i,j} - \frac{\hat{\mathbf{f}}_i(\mathbf{x}) + \hat{\mathbf{f}}_j(\mathbf{x})}{2} - \hat{\mathbf{K}}_{i,j}(\mathbf{x}) \right) \\
&\leq \sum_i \alpha_i^2 \left(\Delta_L \sqrt{\frac{\log(1/\delta)}{2n_i}} + \frac{\Delta_\kappa}{n_i} \right) + \sum_{(i,j) \in [m]^2, i \neq j} \alpha_i \alpha_j \Delta_L \sqrt{\frac{\log(1/\delta)}{8}(n_i^{-1} + n_j^{-1})} \\
&\leq \sum_i \alpha_i^2 \left(\Delta_L \sqrt{\frac{\log(1/\delta)}{2n_i}} + \frac{\Delta_\kappa}{n_i} \right) + \Delta_L \sqrt{\frac{\log(1/\delta)}{8}} \sum_{(i,j) \in [m]^2, i \neq j} \alpha_i \alpha_j (n_i^{-1/2} + n_j^{-1/2}) \\
&= \sum_i \alpha_i^2 \frac{\Delta_\kappa}{n_i} + \Delta_L \sqrt{\frac{\log(1/\delta)}{8}} \sum_{(i,j) \in [m]^2} \alpha_i \alpha_j (n_i^{-1/2} + n_j^{-1/2}) \\
&= \sum_i \alpha_i^2 \frac{\Delta_\kappa}{n_i} + \Delta_L \sqrt{\frac{\log(1/\delta)}{2}} \sum_i \alpha_i n_i^{-1/2} \\
&\leq \sum_i \left(\Delta_L \sqrt{\frac{\log(1/\delta)}{2n_i}} + \frac{\Delta_\kappa}{n_i} \right) \alpha_i.
\end{aligned}$$

The other direction of the inequality is similar.

We finally prove Theorem 2.

Proof: Assume $m \geq 2$, $\beta \geq 4$ and $T \geq 2$. If $T \leq 40m$, then since $T^{-1} \log T$ is decreasing for $T \geq 3$ (the following inequalities are obviously true for $T = 2$),

$$\sqrt{\frac{\beta m \log T}{T}} \geq \sqrt{\frac{4m \log(40m)}{40m}} \geq \sqrt{\frac{\log 80}{10}} \geq 0.66,$$

and Theorem 2 is trivially true since $\mathbb{E}[L(\hat{P}^{(T)})] - \min_{\boldsymbol{\alpha}} L(\boldsymbol{\alpha}) \leq \Delta_L$. Hence we can assume $T \geq 40m + 1$.

Let $\boldsymbol{\alpha}^*$ be the minimizer of $L(\boldsymbol{\alpha})$. Let $\bar{x}^{(t)}$ be the sample obtained at the t -th pull. Let $\alpha_i^{(t-1)} = \mathbf{1}\{t = i\}$ for $t \in [m]$, so “ $\bar{x}^{(t)}$ is generated from the distribution P_i with probability $\alpha_i^{(t-1)}$ ” holds for every $t \geq 1$. Write $\bar{x}^{([s])} := (\bar{x}^{(t)})_{t \in [s]}$. For $s < t$, let $\hat{x}^{(s)}$ be a random variable with the same conditional distribution

given $\bar{x}^{(s-1)}$ as $\bar{x}^{(s)}$, but is conditionally independent of all other random variables given $\bar{x}^{(s-1)}$. The joint distribution of $\bar{x}^{(t-1)}, \bar{x}^{(t)}, \hat{x}^{(s)}$ is

$$P_{\bar{x}^{(t-1)}, \bar{x}^{(t)}, \hat{x}^{(s)}} = P_{\bar{x}^{(t-1)}, \bar{x}^{(t)}} P_{\hat{x}^{(s)} | \bar{x}^{(s-1)}}.$$

Recall that $\bar{x}^{(s)}$ is generated from the distribution P_i with probability $\alpha_i^{(s-1)}$ for $i \in [m]$, where $\boldsymbol{\alpha}^{(s-1)} = (\alpha_i^{(s-1)})_{i \in [m]}$ is computed using $\bar{x}^{(s-1)}$. We have

$$\begin{aligned} & \mathbb{E}[\kappa(\hat{x}^{(s)}, \bar{x}^{(t)})] \\ &= \mathbb{E} \left[\mathbb{E} \left[\kappa(\hat{x}^{(s)}, \bar{x}^{(t)}) \mid \bar{x}^{(t-1)} \right] \right] \\ &\stackrel{(a)}{=} \mathbb{E} \left[\sum_{i=1}^m \sum_{j=1}^m \alpha_i^{(s-1)} \alpha_j^{(t-1)} \mathbb{E}_{X \sim P_i, X' \sim P_j} [\kappa(X, X')] \right] \\ &= \mathbb{E} \left[(\boldsymbol{\alpha}^{(s-1)})^\top \mathbf{K} \boldsymbol{\alpha}^{(t-1)} \right], \end{aligned}$$

where (a) is because $\hat{x}^{(s)}$ only depends on $\bar{x}^{(s-1)}$ (i.e., is conditionally independent of all other random variables in the expression given $\bar{x}^{(s-1)}$), and $\bar{x}^{(t)}$ only depends on $\bar{x}^{(t-1)}$. Write $\delta_{\text{TV}}(A \| B)$ for the total variation distance between the distributions of the random variables A and B . Write $I(A; B | C)$ for the conditional mutual information between A and B given C in nats. We have

$$\begin{aligned} & \mathbb{E}[\kappa(\bar{x}^{(s)}, \bar{x}^{(t)})] \\ &\stackrel{(b)}{\leq} \mathbb{E}[\kappa(\hat{x}^{(s)}, \bar{x}^{(t)})] + \Delta_\kappa \delta_{\text{TV}}(\bar{x}^{(s)}, \bar{x}^{(t)} \| \hat{x}^{(s)}, \bar{x}^{(t)}) \\ &\leq \mathbb{E} \left[(\boldsymbol{\alpha}^{(s-1)})^\top \mathbf{K} \boldsymbol{\alpha}^{(t-1)} \right] + \Delta_\kappa \delta_{\text{TV}}(\bar{x}^{(s-1)}, \bar{x}^{(s)}, \bar{x}^{(t)} \| \bar{x}^{(s-1)}, \hat{x}^{(s)}, \bar{x}^{(t)}) \\ &\stackrel{(c)}{\leq} \mathbb{E} \left[(\boldsymbol{\alpha}^{(s-1)})^\top \mathbf{K} \boldsymbol{\alpha}^{(t-1)} \right] + \Delta_\kappa \sqrt{\frac{1}{2} I(\bar{x}^{(s)}; \bar{x}^{(t)} | \bar{x}^{(s-1)})}, \end{aligned}$$

where (b) is because κ takes values over $[\kappa_0, \kappa_1]$ with $\Delta_\kappa = \kappa_1 - \kappa_0$, and (c) is by Pinsker's inequality. We also have, for every t ,

$$\mathbb{E}[\kappa(\bar{x}^{(t)}, \bar{x}^{(t)})] \leq \mathbb{E} \left[(\boldsymbol{\alpha}^{(t-1)})^\top \mathbf{K} \boldsymbol{\alpha}^{(t-1)} \right] + \Delta_\kappa.$$

Hence,

$$\begin{aligned} & \mathbb{E} \left[\frac{1}{T^2} \sum_{s=1}^T \sum_{t=1}^T \kappa(\bar{x}^{(s)}, \bar{x}^{(t)}) \right] - \mathbb{E} \left[\frac{1}{T^2} \sum_{s=1}^T \sum_{t=1}^T (\boldsymbol{\alpha}^{(s-1)})^\top \mathbf{K} \boldsymbol{\alpha}^{(t-1)} \right] \\ &\leq \frac{2\Delta_\kappa}{T^2} \sum_{s=1}^T \sum_{t=s+1}^T \sqrt{\frac{1}{2} I(\bar{x}^{(s)}; \bar{x}^{(t)} | \bar{x}^{(s-1)})} + \frac{\Delta_\kappa}{T} \\ &= \frac{2\Delta_\kappa}{T^2} \sum_{t=1}^T \sum_{s=1}^{t-1} \sqrt{\frac{1}{2} I(\bar{x}^{(s)}; \bar{x}^{(t)} | \bar{x}^{(s-1)})} + \frac{\Delta_\kappa}{T} \\ &\leq \frac{2\Delta_\kappa}{T^2} \sum_{t=1}^T \sqrt{\frac{t-1}{2} \sum_{s=1}^{t-1} I(\bar{x}^{(s)}; \bar{x}^{(t)} | \bar{x}^{(s-1)})} + \frac{\Delta_\kappa}{T} \\ &\stackrel{(d)}{=} \frac{2\Delta_\kappa}{T^2} \sum_{t=1}^T \sqrt{\frac{t-1}{2} I(\bar{x}^{(t-1)}; \bar{x}^{(t)})} + \frac{\Delta_\kappa}{T} \end{aligned}$$

$$\begin{aligned}
&\stackrel{(e)}{\leq} \frac{2\Delta_\kappa}{T^2} \sum_{t=1}^T \sqrt{\frac{t-1}{2}} \log m + \frac{\Delta_\kappa}{T} \\
&\leq \frac{2\Delta_\kappa}{T^2} \sqrt{\frac{\log m}{2}} \int_0^T \sqrt{\tau} d\tau + \frac{\Delta_\kappa}{T} \\
&= \frac{4\Delta_\kappa}{3} \sqrt{\frac{\log m}{2T}} + \frac{\Delta_\kappa}{T},
\end{aligned}$$

where (d) is by the chain rule of mutual information, and (e) is because $\bar{x}^{(t)}$ only depends on $\bar{x}^{(t-1)}$ through the choice of arm $b^{(t)} \in [m]$, and hence $I(\bar{x}^{(t-1)}; \bar{x}^{(t)})$ is upper bounded by the entropy of $b^{(t)}$, which is at most $\log m$. Also note that $\mathbb{E}[f(\bar{x}^{(t)})] = \mathbf{f}^\top \mathbb{E}[\boldsymbol{\alpha}^{(t-1)}]$. Hence,

$$\begin{aligned}
&\mathbb{E}[L(\hat{P}^{(T)})] \\
&= \mathbb{E} \left[\frac{1}{T} \sum_{t=1}^T f(\bar{x}^{(t)}) + \frac{1}{T^2} \sum_{s=1}^T \sum_{t=1}^T \kappa(\bar{x}^{(s)}, \bar{x}^{(t)}) \right] \\
&\leq \mathbb{E} \left[\frac{1}{T} \sum_{t=1}^T \mathbf{f}^\top \boldsymbol{\alpha}^{(t-1)} + \frac{1}{T^2} \sum_{s=1}^T \sum_{t=1}^T (\boldsymbol{\alpha}^{(s-1)})^\top \mathbf{K} \boldsymbol{\alpha}^{(t-1)} \right] + \frac{4\Delta_\kappa}{3} \sqrt{\frac{\log m}{2T}} + \frac{\Delta_\kappa}{T} \\
&= \mathbb{E} \left[\mathbf{f}^\top \frac{1}{T} \sum_{t=1}^T \boldsymbol{\alpha}^{(t-1)} + \left(\frac{1}{T} \sum_{t=1}^T \boldsymbol{\alpha}^{(t-1)} \right)^\top \mathbf{K} \left(\frac{1}{T} \sum_{t=1}^T \boldsymbol{\alpha}^{(t-1)} \right) \right] + \frac{4\Delta_\kappa}{3} \sqrt{\frac{\log m}{2T}} + \frac{\Delta_\kappa}{T} \\
&= \mathbb{E} \left[L \left(\frac{1}{T} \sum_{t=1}^T \boldsymbol{\alpha}^{(t-1)} \right) \right] + \frac{4\Delta_\kappa}{3} \sqrt{\frac{\log m}{2T}} + \frac{\Delta_\kappa}{T} \\
&\stackrel{(f)}{\leq} \frac{1}{T} \sum_{t=1}^T \mathbb{E} \left[L(\boldsymbol{\alpha}^{(t-1)}) \right] + \frac{4\Delta_\kappa}{3} \sqrt{\frac{\log m}{2T}} + \frac{\Delta_\kappa}{T}, \tag{11}
\end{aligned}$$

where (f) is because \mathbf{K} is positive semidefinite, and hence L is convex. Therefore, to bound the optimality gap, we study the expected loss $\mathbb{E}[L(\boldsymbol{\alpha}^{(t)})]$ of the estimate of the optimal mixture distribution $\boldsymbol{\alpha}^{(t)}$.

Let $\tilde{\delta} > 0$. Let \tilde{E} be the event

$$L(\boldsymbol{\alpha}) - \hat{L}(\boldsymbol{\alpha}; \mathbf{x}^{(n_i)_i}) \leq \sum_{i=1}^m \left(\Delta_L \sqrt{\frac{1}{2n_i} \log \frac{m^2 T^2}{2\tilde{\delta}}} + \frac{\Delta_\kappa}{n_i} \right) \alpha_i$$

for every $n_1, \dots, n_m \in [T]$ and probability vector $\boldsymbol{\alpha}$, as in Lemma 1. By Lemma 1, $\mathbb{P}(\tilde{E}) \geq 1 - \tilde{\delta}$.

Fix a time $t \in \{m, \dots, T\}$. Let E_t be the event

$$\hat{L}(\boldsymbol{\alpha}^*; \mathbf{x}^{(n_i)_i}) - L(\boldsymbol{\alpha}^*) \leq \sum_{i=1}^m \left(\Delta_L \sqrt{\frac{\beta \log t}{2n_i}} + \frac{\Delta_\kappa}{n_i} \right) \alpha_i^*$$

for every $n_1, \dots, n_m \geq 1$ such that $\sum_i n_i = t$. Since

$$\begin{aligned}
&\sum_{i=1}^m \left(\Delta_L \sqrt{\frac{1}{2n_i} \log \frac{m^2 t^2}{2m^2 t^{-2}/2}} + \frac{\Delta_\kappa}{n_i} \right) \alpha_i^* \\
&= \sum_{i=1}^m \left(\Delta_L \sqrt{\frac{1}{2n_i} \log t^4} + \frac{\Delta_\kappa}{n_i} \right) \alpha_i^* \\
&\leq \sum_{i=1}^m \left(\Delta_L \sqrt{\frac{\beta \log t}{2n_i}} + \frac{\Delta_\kappa}{n_i} \right) \alpha_i^*
\end{aligned}$$

by $\beta \geq 4$, applying Lemma 1,

$$\mathbb{P}(E_t) \geq 1 - m^2 t^{-2}/2. \quad (12)$$

If the event E_t holds, by taking $n_i = n_i^{(t)}$,

$$\hat{L}(\boldsymbol{\alpha}^*; \mathbf{x}^{(t)}) - L(\boldsymbol{\alpha}^*) \leq (\boldsymbol{\epsilon}^{(t)})^\top \boldsymbol{\alpha}^*. \quad (13)$$

If the event \tilde{E} holds,

$$\begin{aligned} & L(\boldsymbol{\alpha}) - \hat{L}(\boldsymbol{\alpha}; \mathbf{x}^{(t)}) \\ & \leq \sum_{i=1}^m \left(\Delta_L \sqrt{\frac{1}{2n_i^{(t)}} \log \frac{m^2 T^2}{2\tilde{\delta}}} + \frac{\Delta_\kappa}{n_i^{(t)}} \right) \alpha_i \end{aligned} \quad (14)$$

for every $\boldsymbol{\alpha}$. Combining (13) and (14) (with $\boldsymbol{\alpha} = \boldsymbol{\alpha}^{(t)}$),

$$\begin{aligned} & \hat{L}(\boldsymbol{\alpha}^{(t)}; \mathbf{x}^{(t)}) - \hat{L}(\boldsymbol{\alpha}^*; \mathbf{x}^{(t)}) + (\boldsymbol{\epsilon}^{(t)})^\top \boldsymbol{\alpha}^* \\ & + \sum_{i=1}^m \left(\Delta_L \sqrt{\frac{1}{2n_i^{(t)}} \log \frac{m^2 T^2}{2\tilde{\delta}}} + \frac{\Delta_\kappa}{n_i^{(t)}} \right) \alpha_i^{(t)} \\ & \geq L(\boldsymbol{\alpha}^{(t)}) - L(\boldsymbol{\alpha}^*). \end{aligned}$$

By (6), $\hat{L}(\boldsymbol{\alpha}^{(t)}; \mathbf{x}^{(t)}) - (\boldsymbol{\epsilon}^{(t)})^\top \boldsymbol{\alpha}^{(t)} \leq \hat{L}(\boldsymbol{\alpha}^*; \mathbf{x}^{(t)}) - (\boldsymbol{\epsilon}^{(t)})^\top \boldsymbol{\alpha}^*$, and hence if the events \tilde{E}, E_t hold,

$$\begin{aligned} & (\boldsymbol{\epsilon}^{(t)})^\top \boldsymbol{\alpha}^{(t)} + \sum_{i=1}^m \left(\Delta_L \sqrt{\frac{1}{2n_i^{(t)}} \log \frac{m^2 T^2}{2\tilde{\delta}}} + \frac{\Delta_\kappa}{n_i^{(t)}} \right) \alpha_i^{(t)} \\ & \geq L(\boldsymbol{\alpha}^{(t)}) - L(\boldsymbol{\alpha}^*). \end{aligned} \quad (15)$$

We have

$$\begin{aligned} & (\boldsymbol{\epsilon}^{(t)})^\top \boldsymbol{\alpha}^{(t)} + \sum_{i=1}^m \left(\Delta_L \sqrt{\frac{1}{2n_i^{(t)}} \log \frac{m^2 T^2}{2\tilde{\delta}}} + \frac{\Delta_\kappa}{n_i^{(t)}} \right) \alpha_i^{(t)} \\ & = \sum_{i=1}^m \left(\Delta_L \sqrt{\frac{\beta \log t}{2n_i^{(t)}}} + \frac{\Delta_\kappa}{n_i^{(t)}} + \Delta_L \sqrt{\frac{1}{2n_i^{(t)}} \log \frac{m^2 T^2}{2\tilde{\delta}}} + \frac{\Delta_\kappa}{n_i^{(t)}} \right) \alpha_i^{(t)} \\ & = \sum_i \left(\frac{\Delta_L}{\sqrt{n_i^{(t)}}} \left(\sqrt{\frac{\beta}{2} \log t} + \sqrt{\frac{1}{2} \log \frac{m^2 T^2}{2\tilde{\delta}}} \right) + \frac{2\Delta_\kappa}{n_i^{(t)}} \right) \alpha_i^{(t)} \\ & \leq \sum_i \left(\frac{\Delta_L}{\sqrt{n_i^{(t)}}} \left(\sqrt{\frac{\beta}{2} \log T} + \sqrt{\frac{1}{2} \log \frac{m^2 T^2}{2\tilde{\delta}}} \right) + \frac{\Delta_L}{\sqrt{n_i^{(t)}}} \right) \alpha_i^{(t)} \\ & = \Delta_L \eta \sum_i \frac{\alpha_i^{(t)}}{\sqrt{n_i^{(t)}}}, \end{aligned}$$

where

$$\eta := \sqrt{\frac{\beta}{2} \log T} + \sqrt{\frac{1}{2} \log \frac{m^2 T^2}{2\tilde{\delta}}} + 1.$$

Substituting into (15), if the events \tilde{E}, E_t hold,

$$\Delta_L \eta \sum_i \frac{\alpha_i^{(t)}}{\sqrt{n_i^{(t)}}} \geq L(\boldsymbol{\alpha}^{(t)}) - L(\boldsymbol{\alpha}^*).$$

Hence, in general (regardless of whether \tilde{E}, E_t hold), denoting the indicator function of $\tilde{E} \cap E_t$ as $\mathbf{1}_{\tilde{E} \cap E_t} \in \{0, 1\}$,

$$\sum_i \frac{\alpha_i^{(t)}}{\sqrt{n_i^{(t)}}} \geq \frac{L(\boldsymbol{\alpha}^{(t)}) - L(\boldsymbol{\alpha}^*)}{\Delta_L \eta} \mathbf{1}_{\tilde{E} \cap E_t}.$$

Let

$$\Psi^{(t)} := \sum_{i=1}^m \psi(n_i^{(t)} - 1),$$

where $\psi(n) := \sum_{i=1}^n i^{-1/2}$. Recall that we pull arm i at time $t+1$ with probability $\alpha_i^{(t)}$. The expected increase of $\Psi^{(t)}$ is

$$\begin{aligned} \mathbb{E} \left[\Psi^{(t+1)} - \Psi^{(t)} \mid \mathbf{x}^{(t)} \right] &= \sum_{i=1}^m \left(\psi(n_i^{(t)}) - \psi(n_i^{(t)} - 1) \right) \alpha_i^{(t)} \\ &= \sum_{i=1}^m \frac{\alpha_i^{(t)}}{\sqrt{n_i^{(t)}}} \\ &\geq \frac{L(\boldsymbol{\alpha}^{(t)}) - L(\boldsymbol{\alpha}^*)}{\Delta_L \eta} \mathbf{1}_{\tilde{E} \cap E_t}. \end{aligned}$$

Note that

$$\begin{aligned} \Psi^{(T)} &= \sum_{i=1}^m \psi(n_i^{(T)} - 1) \\ &\leq \sum_{i=1}^m \int_0^{n_i^{(T)} - 1} \min\{\tau^{-1/2}, 1\} d\tau \\ &\stackrel{(a)}{\leq} m \int_0^{m^{-1} \sum_{i=1}^m n_i^{(T)} - 1} \min\{\tau^{-1/2}, 1\} d\tau \\ &= m \int_0^{T/m - 1} \min\{\tau^{-1/2}, 1\} d\tau \\ &\stackrel{(b)}{=} m \left(1 + \int_1^{T/m - 1} \tau^{-1/2} d\tau \right) \\ &= m \left(2\sqrt{\frac{T}{m}} - 1 - 1 \right), \end{aligned}$$

where (a) is because $a \mapsto \int_0^a \min\{\tau^{-1/2}, 1\} d\tau$ is concave, and (b) is because $T \geq 40m + 1$, so $T/m - 1 \geq 1$. Therefore,

$$\begin{aligned} m \left(2\sqrt{\frac{T}{m}} - 1 - 1 \right) &\geq \mathbb{E} \left[\Psi^{(T)} - \Psi^{(m)} \right] \\ &= \sum_{t=m}^{T-1} \mathbb{E} \left[\Psi^{(t+1)} - \Psi^{(t)} \right] \\ &\geq \sum_{t=m}^{T-1} \mathbb{E} \left[\frac{L(\boldsymbol{\alpha}^{(t)}) - L(\boldsymbol{\alpha}^*)}{\Delta_L \eta} \mathbf{1}_{\tilde{E} \cap E_t} \right] \\ &\geq \frac{1}{\Delta_L \eta} \sum_{t=m}^{T-1} \left(\mathbb{E} \left[L(\boldsymbol{\alpha}^{(t)}) - L(\boldsymbol{\alpha}^*) \right] - \Delta_L \mathbb{P}((\tilde{E} \cap E_t)^c) \right) \end{aligned}$$

$$\begin{aligned}
&\stackrel{(c)}{\geq} \frac{1}{\Delta_L \eta} \sum_{t=m}^{T-1} \left(\mathbb{E} \left[L(\boldsymbol{\alpha}^{(t)}) - L(\boldsymbol{\alpha}^*) \right] - \Delta_L (\tilde{\delta} + m^2 t^{-2}/2) \right) \\
&\geq \frac{1}{\Delta_L \eta} \sum_{t=m}^{T-1} \mathbb{E} \left[L(\boldsymbol{\alpha}^{(t)}) - L(\boldsymbol{\alpha}^*) \right] - \frac{T\tilde{\delta}}{\eta} - \frac{m^2}{2\eta} \int_{m-1}^{T-1} t^{-2} dt \\
&\geq \frac{1}{\Delta_L \eta} \sum_{t=m}^{T-1} \mathbb{E} \left[L(\boldsymbol{\alpha}^{(t)}) - L(\boldsymbol{\alpha}^*) \right] - \frac{T\tilde{\delta}}{\eta} - \frac{m^2}{2\eta(m-1)} \\
&\geq \frac{1}{\Delta_L \eta} \sum_{t=m}^{T-1} \mathbb{E} \left[L(\boldsymbol{\alpha}^{(t)}) - L(\boldsymbol{\alpha}^*) \right] - \frac{T\tilde{\delta}}{\eta} - \frac{m}{\eta},
\end{aligned}$$

where (c) is by (12). Hence,

$$\begin{aligned}
&\frac{1}{\Delta_L} \sum_{t=0}^{T-1} \mathbb{E} \left[L(\boldsymbol{\alpha}^{(t)}) - L(\boldsymbol{\alpha}^*) \right] \\
&\leq \frac{1}{\Delta_L} \sum_{t=m}^{T-1} \mathbb{E} \left[L(\boldsymbol{\alpha}^{(t)}) - L(\boldsymbol{\alpha}^*) \right] + m \\
&\leq \eta m \left(2\sqrt{\frac{T}{m}} - 1 - 1 \right) + T\tilde{\delta} + 2m \\
&\stackrel{(d)}{=} m \left(2\sqrt{\frac{T}{m}} - 1 - 1 \right) \left(\sqrt{\frac{\beta}{2}} \log T + \sqrt{\frac{1}{2}} \log \frac{mT^3}{2} + 1 \right) + 3m \\
&\stackrel{(e)}{\leq} m \left(2\sqrt{\frac{T}{m}} - 1 \right) \left(\sqrt{\frac{\beta}{2}} \log T + \sqrt{\frac{1}{2}} \log \frac{mT^3}{2} + 1 \right) \\
&\leq 2\sqrt{mT} \left(\sqrt{\frac{\beta}{2}} \log T + \sqrt{\frac{1}{2}} \log \frac{mT^3}{2} + 1 \right),
\end{aligned}$$

where (d) is by substituting $\tilde{\delta} = m/T$, (e) is because $\sqrt{\frac{\beta}{2}} \log T \geq \sqrt{2 \log 81} \geq 2.9$ and $\sqrt{\frac{1}{2}} \log \frac{mT^3}{2} \geq 2.5$ (recall that $T \geq 40m + 1 \geq 81$). Substituting into (11),

$$\begin{aligned}
&\frac{1}{\Delta_L} \left(\mathbb{E}[L(\hat{P}^{(T)})] - L(\boldsymbol{\alpha}^*) \right) \\
&\leq \frac{1}{\Delta_L T} \sum_{t=1}^T \mathbb{E} \left[L(\boldsymbol{\alpha}^{(t-1)}) - L(\boldsymbol{\alpha}^*) \right] + \frac{4\Delta_\kappa}{3\Delta_L} \sqrt{\frac{\log m}{2T}} + \frac{\Delta_\kappa}{T\Delta_L} \\
&\leq 2\sqrt{\frac{m}{T}} \left(\sqrt{\frac{\beta}{2}} \log T + \sqrt{\frac{1}{2}} \log \frac{mT^3}{2} + 1 \right) + \frac{2}{3} \sqrt{\frac{\log m}{2T}} + \frac{1}{2T} \\
&= \frac{1}{\sqrt{T}} \left(2\sqrt{\frac{\beta}{2}} m \log T + \sqrt{2m \log \frac{mT^3}{2}} + 2\sqrt{m} + \frac{2}{3} \sqrt{\frac{\log m}{2}} + \frac{1}{2\sqrt{T}} \right) \\
&\leq \frac{1}{\sqrt{T}} \left(2\sqrt{\frac{\beta}{2}} m \log T + \sqrt{2m \log T^4} + \frac{2\sqrt{m \log T}}{\sqrt{\log 81}} \right. \\
&\quad \left. + \frac{2}{3} \frac{\sqrt{m \log T}}{\sqrt{m \log(40m+1)}} \sqrt{\frac{\log m}{2}} + \frac{1}{2\sqrt{81}} \cdot \frac{\sqrt{m \log T}}{\sqrt{2 \log 81}} \right) \\
&= \sqrt{\frac{m \log T}{T}} \left(\sqrt{2\beta} + 2\sqrt{2} + \frac{2}{\sqrt{\log 81}} + \frac{2}{3} \sqrt{\frac{\log m}{2m \log(40m+1)}} + \frac{1}{2\sqrt{81}} \cdot \frac{1}{\sqrt{2 \log 81}} \right)
\end{aligned}$$

$$\begin{aligned}
&\leq \sqrt{\frac{m \log T}{T}} \left(\sqrt{2\beta} + 2\sqrt{2} + \frac{2}{\sqrt{\log 81}} + \frac{2}{3} \sqrt{\frac{\log 2}{4 \log 81}} + \frac{1}{2\sqrt{81}} \cdot \frac{1}{\sqrt{2 \log 81}} \right) \\
&\leq \sqrt{\frac{m \log T}{T}} (\sqrt{2\beta} + 3.934) \\
&\leq \sqrt{\frac{m \log T}{T}} \left(\sqrt{2\beta} + \frac{3.934}{2} \sqrt{\beta} \right) \\
&\leq 3.382 \sqrt{\frac{\beta m \log T}{T}}.
\end{aligned}$$

This completes the proof of Theorem 2 (with an improved constant 3.382 instead of 4).

B Sparse Mixture Upper Confidence Bound-Continuum-Armed Bandit Algorithm

Algorithm 3 Sparse-Mixture-UCB-CAB

- 1: **Input:** m generative arms, number of rounds T
- 2: **Output:** Gathered samples $\mathbf{x}^{(T)}$
- 3: Initialize the set of subscribed arms $\mathcal{S} \leftarrow [m]$.
- 4: **for** $t \in \{0, \dots, m-1\}$ **do**
- 5: Pull arm $t+1$ at time $t+1$ to obtain sample $x_{t+1,1} \sim P_{t+1}$. Set $n_{t+1}^{(m)} = 1$.
- 6: **end for**
- 7: **for** $t \in \{m, \dots, T-1\}$ **do**
- 8: **repeat**
- 9: Compute

$$\boldsymbol{\alpha}^{(t)} \leftarrow \underset{\boldsymbol{\alpha}: \text{supp}(\boldsymbol{\alpha}) \subseteq \mathcal{S}}{\text{argmin}} \left(\hat{L}(\boldsymbol{\alpha}; \mathbf{x}^{(t)}) + \lambda |\mathcal{S}| - (\boldsymbol{\epsilon}^{(t)})^\top \boldsymbol{\alpha} \right), \tag{16}$$

where $\boldsymbol{\epsilon}^{(t)} \in \mathbb{R}^m$ is defined in (7). Let the minimum value above be C .

- 10: Compute the following “worst arm” if $|\mathcal{S}| \geq 2$:

$$i' \leftarrow \underset{i \in \mathcal{S}}{\text{argmin}} \min_{\boldsymbol{\alpha}: \text{supp}(\boldsymbol{\alpha}) \subseteq \mathcal{S} \setminus \{i\}} \left(\hat{L}(\boldsymbol{\alpha}; \mathbf{x}^{(t)}) + \lambda (|\mathcal{S}| - 1) + (\boldsymbol{\epsilon}^{(t)})^\top \boldsymbol{\alpha} \right).$$

Let the minimum value above be C' .

- 11: **if** $C' \leq C$ **then**
 - 12: Unsubscribe arm i' (i.e., $\mathcal{S} \leftarrow \mathcal{S} \setminus \{i'\}$)
 - 13: **end if**
 - 14: **until** no more arms are unsubscribed
 - 15: Generate the arm index $b^{(t+1)} \in [m]$ at random with $\mathbb{P}(b^{(t+1)} = i) = \alpha_i^{(t)}$.
 - 16: Pull arm $b = b^{(t+1)}$ at time $t+1$ to obtain a new sample $x_{b, n_b^{(t)}+1} \sim P_b$. Set $n_b^{(t+1)} = n_b^{(t)} + 1$ and $n_j^{(t+1)} = n_j^{(t)}$ for $j \neq b$.
 - 17: **end for return** samples $\mathbf{x}^{(T)}$
-

C Additional Numerical Results

C.1 Details of the Numerical Experiments

Hyper-parameter Choice. The kernel bandwidths for the RKE and KID metrics were chosen based on the guidelines provided in their respective papers to ensure clear distinction between models. The values for Δ_L and Δ_κ in our online algorithms (7) were set according to the magnitudes of the metrics and their behavior on a validation subset. The number of sampling rounds was adjusted according to the number of models and metric convergence, both of which depend on the bandwidth. To ensure the statistical significance of results, all experiments were repeated 10 times with different random seeds, and the reported plots represent the average results.

C.2 Optimal Mixture for Quality and Diversity via KID

Suppose P is the distribution of generated images of a model, and Q is the target distribution. Recall that for KID (3), we take the quadratic term to be $\kappa(x, x') = k(\psi(x), \psi(x'))$ (with an expectation $\mathbb{E}_{X, X' \sim P}[k(\psi(X), \psi(X'))]$) and the linear term to be $f(x) = -2\mathbb{E}_{Y \sim Q}[k(\psi(x), \psi(Y))]$ (with an expectation $-2\mathbb{E}_{X \sim P, Y \sim Q}[k(\psi(X), \psi(Y))]$). In order to run our online algorithms, we use Δ_L and Δ_κ based on a validation portion to make sure the UCB terms have the right magnitude for forcing exploration.

FFHQ Generated Images. In this experiment, we use images generated by five different models: LDM [36], StyleGAN-XL [37], Efficient-vdVAE [38], Insgen [39], and StyleNAT [40]. We use 10,000 images from each model and a kernel bandwidth of 40 to determine the optimal mixture, resulting in the weights (0.33, 0.57, 0, 0, 0.10). The online algorithms run for 8,000 sampling rounds. The quality and diversity scores for each model, including the results for the optimal mixture based on KID, are presented in Table 1.

In Tables 1 and 2, we observe that the Precision of the optimal mixture is similar to that of the maximum Precision score among individual models. On the other hand, the Recall-based diversity improved in the mixture case. However, the quality-measuring Density score slightly decreased for the selected mixture model, as Density is a linear score for quality that could be optimized by an individual model. On the other hand, the Coverage score of the mixture model was higher than each individual model.

Note that Precision and Density are scores on the average quality of samples. Intuitively, the quality score of a mixture of models is the average of the quality score of the individual models, and hence the quality score of a mixture cannot be better than the best individual model. On the other hand, Recall and Coverage measure the diversity of the samples, which can increase by considering a mixture of the models. To evaluate the net diversity-quality effect, we measured the FID score of the selected mixture and the best individual model, and the selected mixture model had a better FID score compared to the individual model with the best FID.

Model	Precision \uparrow	Recall \uparrow	Density \uparrow	Coverage \uparrow	FID \downarrow
LDM	0.856 \pm 0.008	0.482 \pm 0.008	0.959 \pm 0.027	0.776 \pm 0.006	189.876 \pm 1.976
StyleGAN-XL	0.798 \pm 0.007	0.515 \pm 0.007	0.726 \pm 0.018	0.691 \pm 0.009	186.163 \pm 2.752
Efficient-vdVAE	0.854 \pm 0.011	0.143 \pm 0.007	0.952 \pm 0.033	0.545 \pm 0.008	490.385 \pm 4.377
Insgen	0.76 \pm 0.006	0.281 \pm 0.007	0.716 \pm 0.016	0.692 \pm 0.005	278.235 \pm 1.617
StyleNAT	0.834 \pm 0.008	0.478 \pm 0.007	0.867 \pm 0.023	0.775 \pm 0.007	185.067 \pm 2.123
Optimal Mixture (KID)	0.818 \pm 0.007	0.57 \pm 0.008	0.816 \pm 0.025	0.765 \pm 0.007	168.127 \pm 1.596
Mixture-UCB-CAB (KID)	0.828 \pm 0.007	0.571 \pm 0.008	0.838 \pm 0.016	0.787 \pm 0.007	170.578 \pm 2.075
Mixture-UCB-OGD (KID)	0.827 \pm 0.006	0.573 \pm 0.005	0.825 \pm 0.015	0.787 \pm 0.006	170.113 \pm 1.930

Table 1: Quality and diversity scores for the FFHQ experiment, including precision, recall, density, coverage, and FID metrics (\pm standard deviation).

LSUN-Bedroom We use images generated by four different models: StyleGAN [41], Projected GAN [42], iDDPM [43], and Unleashing Transformers [44]. We utilize 10,000 images from each model to calculate the optimal mixture, resulting in weights of (0.51, 0, 0.49, 0). A kernel bandwidth of 40 is used and the algorithms run for 8,000 sampling steps. The quality and diversity scores for each model, including the results for the optimal mixture based on KID, are presented in Table 2.

Model	Precision \uparrow	Recall \uparrow	Density \uparrow	Coverage \uparrow	FID \downarrow
StyleGAN	0.838 ± 0.008	0.446 ± 0.007	0.941 ± 0.019	0.821 ± 0.004	175.575 ± 2.055
Projected GAN	0.749 ± 0.015	0.329 ± 0.008	0.592 ± 0.027	0.517 ± 0.008	324.066 ± 3.753
iDDPM	0.838 ± 0.006	0.641 ± 0.006	0.660 ± 0.018	0.825 ± 0.006	154.680 ± 3.036
Unleashing Transformers	0.786 ± 0.008	0.449 ± 0.006	0.649 ± 0.013	0.581 ± 0.013	339.982 ± 6.118
Optimal Mixture (KID)	0.838 ± 0.006	0.589 ± 0.005	0.900 ± 0.016	0.833 ± 0.004	149.779 ± 2.238
Mixture-UCB-CAB (KID)	0.835 ± 0.007	0.602 ± 0.007	0.894 ± 0.014	0.834 ± 0.005	151.28 ± 1.801
Mixture-UCB-OGD (KID)	0.838 ± 0.008	0.599 ± 0.007	0.902 ± 0.023	0.834 ± 0.006	151.10 ± 1.906

Table 2: Quality and diversity scores for the LSUN-Bedroom experiment, including precision, recall, density, coverage, and FID metrics (\pm standard deviation).

Truncated FFHQ. We use StyleGAN2-ADA [47] trained on FFHQ dataset to generate images. We randomly choose 8 initial points and use the Truncation Method [41, 46] to generate images with limited diversity around each of the chosen points. We use truncation value of 0.3 and generate 5000 images from each model to find the optimal mixture. The optimal weights for the mixture is (0.07, 0.28, 0.10, 0.04, 0.21, 0.11, 0.12, 0.07). A kernel bandwidth of 40 is used and 4,000 sampling steps are conducted.

C.3 Optimal Mixture for Diversity via RKE

Truncated FFHQ. We employ StyleGAN2-ADA [47], trained on the FFHQ dataset, to generate images. Eight initial points are randomly selected, and the Truncation Method [41, 46] is applied with a truncation value of 0.3 to generate images with limited diversity around these points. For the offline optimization, 5,000 images are generated from each model, using a kernel bandwidth of 40 to identify the optimal mixture. In the online experiment, sampling is conducted over 2,000 steps.

Truncated AFHQ Cat. Similar to the previous experiment, we use StyleGAN2-ADA to generate AFHQ Cat images. Four initial points are selected, and a truncation value of 0.6 is applied to simulate diversity-controlled models. For the quadratic optimization, 5,000 images are generated from each model, with sampling over 1,200 steps to determine the optimal mixture.

Style-Specific Generators. We use Stable Diffusion XL to generate images of cars in distinct styles: realistic, surreal, and cartoon. For this experiment, we utilize 2,000 images from each model to determine the optimal mixture, which yields weights of (0.67, 0.27, 0.06). This mixture increases the RKE value from 7.86 (the optimal value of the realistic images) to 9.19. We set the kernel bandwidth to 30 and execute the online algorithms over 1,000 sampling steps.

Sofa Images. We generate images of the object ‘‘Sofa’’ using prompts with descriptions of the environment across the models FLUX.1-Schnell [50], Kandinsky 3.0 [51], PixArt- α [52], and Stable Diffusion XL [49]. Solving the RKE optimization with 1,000 images reveals that sampling 38% from FLUX and 62% from Kandinsky improves the RKE score from the one-arm optimum of 12.12 to 14.51. We set the kernel bandwidth to 30 and conduct the online experiment over 700 steps. We observe that Mixture-UCB-OGD achieves noticeably faster convergence to the optimal mixture RKE in this scenario.

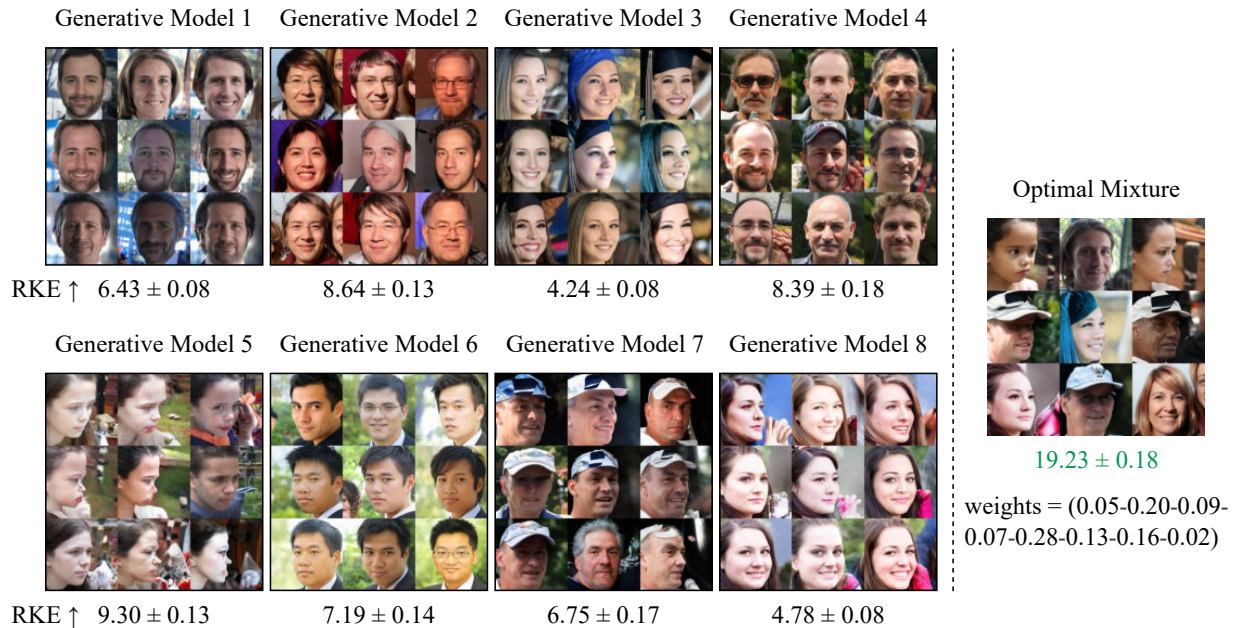


Figure 8: Visual demonstration of the increase in diversity when mixing arms compared to individual arms for truncated FFHQ generative models. The RKE values for each model and the mixture serve as indicators of diversity.

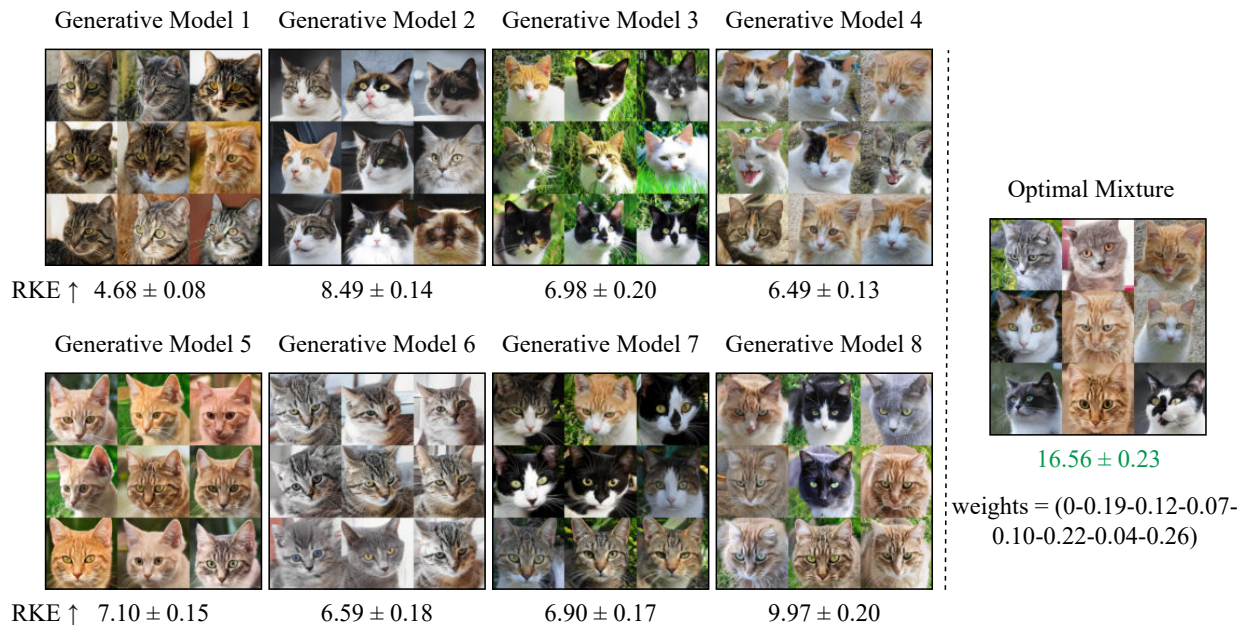


Figure 9: Visual demonstration of the increase in diversity when mixing arms compared to individual arms for truncated AFHQ Cat generative models. The RKE values for each model and the mixture represent the diversity.

The prompts follow the structure: “A *adjective* sofa is *verb* in a *location*,” with the terms for Adjective, Verb, and Location generated by GPT-4o [59], specifically for the object ”Sofa.”



Figure 10: Visual comparison of diversity of each arm and the mixture for sofa image generators

Red Bird Images. To observe the performance of mixing the models while generating images on a single prompt, we generate images with the prompt “Red bird, cartoon style” using Kandinsky 3.0 [51], Stable Diffusion 3-medium [53], and PixArt- α [52]. We use 8000 images and a kernel bandwidth of 30 to find the optimal mixture in an offline manner. The increase in diversity is shown in Figure 1. We observe a noticeable boost in the RKE and Vendi scores, showing the diversity has improved. The performance of our online algorithms and the comparison of samples generated by each online algorithm are shown in Figure 2.

Dog Breeds Images. Stable Diffusion XL is used to generate images of three breeds of dogs: Poodle, Bulldog, and German Shepherd. As shown in Figure 5, using a mixture of models results in an increase in mode count from 1.5 to 3, supporting our claim of enhanced diversity. We set the kernel bandwidth to 50 and generate 1,000 images for each breed to determine the optimal mixture, which was (0.33, 0.31, 0.36). The online algorithms are executed for 500 sampling steps.

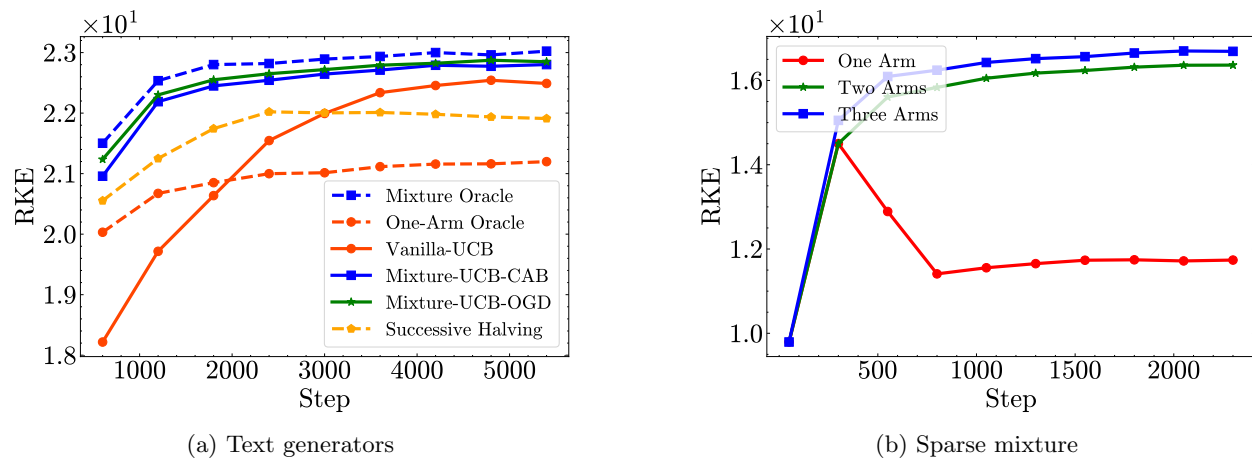


Figure 11: Comparison of online algorithms for the RKE metric on text generative models and the Sparse Mixture algorithm for FFHQ truncated generators

Text Generative Models We utilize the OpenLLMText dataset [54], which consists of 60,000 human texts rephrased paragraph by paragraph using the models GPT2-XL [55], LLaMA-7B [56], and PaLM [57]. To extract features from each text, we employ the RoBERTa text encoder [35]. By solving the optimization problem on 10,000 texts from each model, we find that mixing the models with probabilities (0.02, 0.34, 0.64, 0) achieves the optimal mixture, improving the RKE from an optimal single model score of 69.3 to 75.2. A bandwidth of 0.6 is used for the kernel, and we run the online algorithms for 7,000 steps to demonstrate their performance.

Sparse Mixture Four different initial points and StyleGAN2-ADA are used to generate images with a truncation of 0.6 around the points, simulating diversity-controlled models. A value of $\lambda = 0.06$ and a bandwidth of 30 are selected based on the magnitudes of RKEs from the validation dataset to determine when to “unsubscribe” models in the Sparse-Mixture-UCB-CAB algorithm. We conduct three scenarios, gradually reducing the number of models to between one and three, and present a comparison of the resulting plots and their convergence values in Figure 11b.

C.4 Optimal Mixture for Diversity and Quality via RKE and Precision/Density

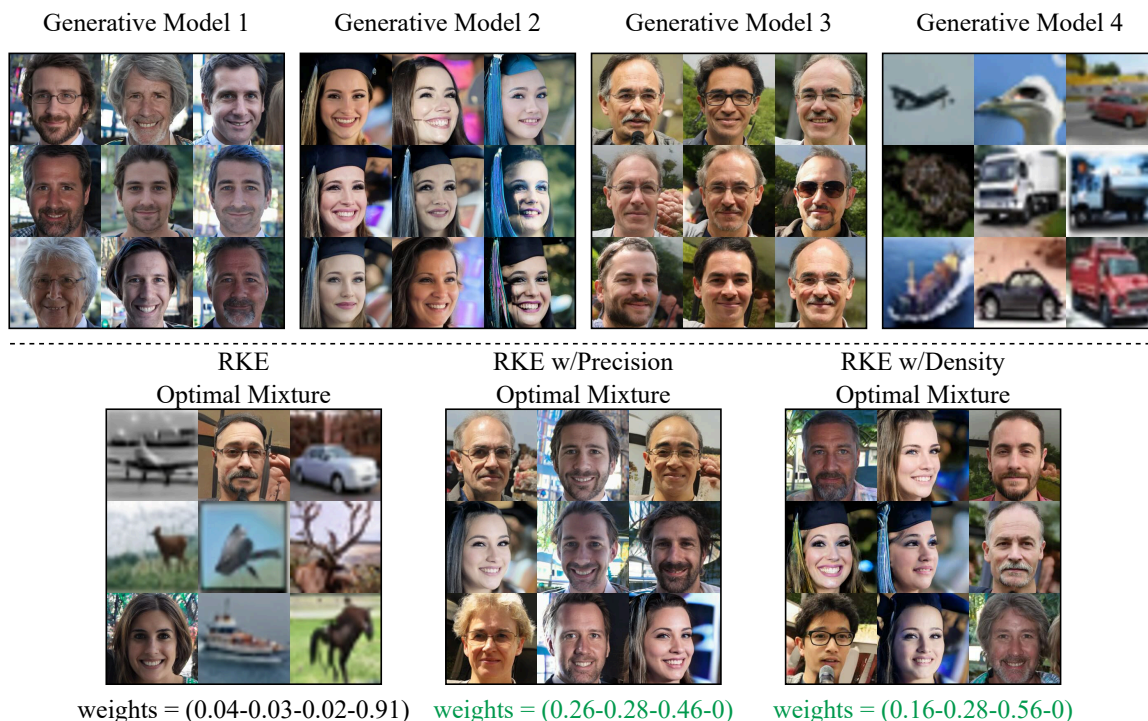


Figure 12: Visual demonstration of the effect of combining Precision/Density with RKE. The CIFAR10 generator is excluded when these quality metrics are applied.

In this experiment, we use four arms: three of them are StyleGAN2-ADA models trained on FFHQ, each using a truncation value of 0.3 around a randomly selected point. The fourth arm is StyleGAN2-ADA trained on CIFAR-10. We generated 5,000 images and use a kernel bandwidth of 30 to calculate the optimal mixture. When optimizing purely for diversity using the RKE metric, the high diversity of the fourth model leads to a

probability of 0.91 being assigned to it, as shown in Figure 12. However, despite the increased diversity, the quality of the generated images, based on the reference distribution, is unsatisfactory.

To address this, we incorporate a quality metric, specifically Precision/Density, into the optimization. We use the RKE score as \mathbf{K} and the weighted Precision/Density as \mathbf{f} according to equation 5. The weights for the quality metrics ($\lambda = 0.2$ and 0.5) are selected based on validation data to ensure comparable scaling between the two metrics. As a result, Figure 12 shows that the fourth arm, which has low-quality outputs, is assigned a weight of zero. The online algorithms also run for 4,000 steps, with the results depicted in Figure 7.